Steel and Composite Structures, *Vol. 25, No. 2 (2017) 141-155*
DOI: https://doi.org/10.12989/scs.2017.25.2.141

Damping and vibration analysis of viscoelastic curved microbeam reinforced with FG-CNTs resting on viscoelastic medium using strain gradient theory and DQM

Farshid Allahkarami [1], Mansour Nikkhah-Bahrami [*1] and Maryam Ghassabzadeh Saryazdi [2]

[1] *Department of Mechanical and Aerospace Engineering, Science and Research Branch, Islamic Azad University, Tehran, Iran*
[2] *Vehicle Technology Research Institute, Amirkabir University of Technology, Tehran, Iran*

(*Received March 24, 2017, Revised May 17, 2017, Accepted June 21, 2017*)

Abstract. This paper presents an investigation into the magneto-thermo-mechanical vibration and damping of a viscoelastic functionally graded-carbon nanotubes (FG-CNTs)-reinforced curved microbeam based on Timoshenko beam and strain gradient theories. The structure is surrounded by a viscoelastic medium which is simulated with spring, damper and shear elements. The effective temperature-dependent material properties of the CNTs-reinforced composite beam are obtained using the extended rule of mixture. The structure is assumed to be subjected to a longitudinal magnetic field. The governing equations of motion are derived using Hamilton's principle and solved by employing differential quadrature method (DQM). The effect of various parameter like volume percent and distribution type of CNTs, temperature change, magnetic field, boundary conditions, material length scale parameter, central angle, viscoelastic medium and structural damping on the vibration and damping behaviors of the nanocomposite curved microbeam is examined. The results show that with increasing volume percent of CNTs and considering magnetic field, material length scale parameter and viscoelastic medium, the frequency of the system increases and critically damped situation occurs at higher values of damper constant. In addition, the structure with FGX distribution type of CNTs has the highest stiffness. It is also observed that increasing temperature, structural damping and central angle of curved microbeam decreases the frequency of the system.

Keywords: vibration analysis; FG-CNTs-reinforced composite; curved microbeam; Timoshenko beam; strain gradient theory; magnetic field; viscoelastic medium

1. Introduction

During last two decades, the need to design the high performance and efficiency structures with low dimensions has attracted the researchers to study the nano/micro electromechanical systems (MEMS/NEMS) which incorporate the structural elements like beams, plates and membranes in micro/nano scale. Curved beams are one types of beam which are used in micro and nano-scale devices and systems such as biosensors, atomic force microscopes (AFM), micro/nano-electromechanical systems (MEMS/NEMS), civil and aerospace engineering. In order to better understand the behavior of these systems, the theoretical analysis and numerical methods play a significant role in capturing the size effects on the static and dynamic responses. Many investigations have been done by researchers using the size-dependent theories. For example, dynamic analysis of an embedded single-walled carbon nanotube (SWCNT) traversed by a moving nanoparticle, which was modeled as a moving load, was investigated by Şimşek (2011) based on the nonlocal Timoshenko beam theory, including transverse shear deformation and rotary inertia. Yang *et al*. (2017) presented a size-dependent mathematical model of a FG-CNTs- reinforced microbeam based on the nonlocal stress and strain gradient theories. They studied nonlinear dynamic behavior of the microbeam subjected to electrostatic, piezoelectric actuation and thermal loading. Ebrahimi and Salari (2015) sought thermal buckling and free vibration analysis of the functionally graded (FG) nanobeams in thermal environments. They developed the size-dependent model of the nanobeam based on Timoshenko beam theory and considered the structure subjected to an in-plane thermal loading. Ghadiri and Shafiei (2016) analyzed vibration behavior of rotating FG microbeam based on modified couple stress theory. They also used Timoshenko beam theory and considered different temperature distributions. Ilkhani and Hosseini-Hashemi (2016) also applied modified couple stress theory to proposed size-dependent vibro-buckling analysis of a rotating beam. They derived the equations of motion by combining Euler-Bernoulli and Timoshenko beam theories and studied the effects of scale parameter, rotational speed, tangential load value and direction. In addition, Dehrouyeh-Semnani *et al*. (2015) presented a size-dependent mathematical formulation of a FG viscoelastically damped sandwich microbeam based on modified couple stress theory. They used Navier's solution method to examine the influence of material length scale parameter, power index and loss factor ratios on the natural frequency. Zenkour and Abouelregal (2016) investigated the vibration phenomenon

*Corresponding author, Professor,
E-mail: mbahrami@ut.ac.ir
[a] Ph.D. Student
[b] Assistant Professor

ISSN: 1229-9367 (Print), 1598-6233 (Online)

of a nanobeam subjected to a time-dependent heat flux. The vibration analysis of a cantilever microbeam is applied by Abdollahi *et al*. (2016). Chen and Meguid (2015) investigated the effects of boundary condition, residual axial force, arch shape and temperature changes on the buckling behavior of a curved microbeam. They developed the governing equations using Euler-Bernoulli beam theory and solved them applying Galerkin decomposition approach. Ghayesh *et al*. (2017) sought the vibration behavior of a geometrically imperfect shear-deformable microbeam. They considered all the translational and rotational displacements and developed the mathematical formulation based on the modified couple stress theory Also, Şimşek (2015) analyzed the nonlinear vibration behavior of an axially functionally graded (AFG) microbeam by developing a size-dependent theoretical model based on the Euler-Bernoulli and modified couple stress theories. He used Galerkin approach to examine the effects of the length scale parameter, vibration amplitude, boundary conditions and material variation on the frequencies of the structure. Also, Wang *et al*. (2013) studied the size-dependent vibration behavior of a three-dimensional cylindrical microbeams using modified couple stress. They considered only one single material length scale parameter. Tang *et al*. (2014) and Shafiei *et al*. (2016) are the other researchers which employed modified couple stress theory to capture the size effect on the vibrational behavior of the microbeams. A size-dependent model for the free vibration analysis of FG microbeams based on strain gradient theory is proposed by Ansari *et al*. (2011). They assumed the material properties to be graded along the thickness direction on the basis of Mori-Tanaka approach. Ghayesh *et al*. (2016) studied the viscoelastically coupled size-dependent dynamics of the microbeams using Kelvin-Voigt viscoelastic model. Zamanian and Karimiyan (2015) presented the bending and vibration analysis of a doubled microbeam under electrostatic actuation. A non-classical beam model based on the Eringen's nonlocal elasticity theory was proposed by Şimşek (2014) for nonlinear vibration of nanobeams with axially immovable ends. Jia *et al*. (2015) sought the size effect on the free vibration behavior of the FG microbeams under combined electro-static force, temperature change and Casimir force. A nonlocal trigonometric shear deformation beam theory based on neutral surface position was developed by Ahouel *et al*. (2016) for bending, buckling, and vibration of functionally graded (FG) nanobeams using the nonlocal differential constitutive relations of Eringen. Togun and Bağdatli (2016) presented a nonlinear vibration analysis of the tensioned nanobeams with simple–simple and clamped–clamped boundary conditions. The size dependent Euler–Bernoulli beam model was applied to tensioned nanobeam.

To the best of authors' knowledge, magneto-thermo-mechanical vibration and damping analysis of a FG-CNTs-reinforced curved microbeam resting on viscoelastic medium is not reported in available literature. The structure is considered subjected to magnetic loads. Timoshenko beam and strain gradient theories are employed to develop the mathematical formulation which is able to capture the small scale effects. The equivalent mechanical properties of the microbeam are obtained using the extended rule of mixture. Also, the governing equations are derived based on the energy method and using Hamilton's principle. The imaginary and real parts of eigenfrequency and damping ratio of the system are obtained using DQM and the effects of parameters such as structural damping, boundary conditions, viscoelastic medium, volume percent and distribution types of CNTS, magnetic field, material length scale parameters, temperature change and central angle of the curved microbeam are studied on the vibration and damping analysis of system.

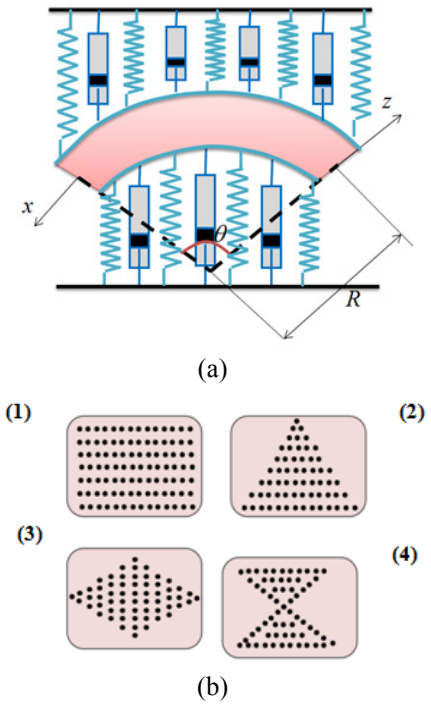

Fig. 1 (a) A schematic of FG-CNT reinforced curved micro beam; (b) different distribution of CNTs (1) UD; (2) FGA; (3) FGO; (4) FGX

2. Geometry of problem

A FG-CNTs-reinforced curved microbeam of length L, radius R and thickness h is illustrated in Fig. 1(a).

The microbeam is surrounded by a viscoelastic medium which is modeled with spring, damper and shear elements. Different types of CNTs distribution, including UD, FGA, FGO and FGX are considered which are shown in Fig. 1(b).

3. Theories and mathematical formulation

3.1 Extended rule of mixture

The effective material properties of the CNTs-reinforced composite beam are obtained by employing the extended rule of mixture. According to this method, the CNTs are assumed as short fibers which are aligned and straight. Hence, the effective Young's modulus and shear modulus of the CNTs-reinforced composite beam can be expressed as (Zhang *et al*. 2015)

$$E_{11} = \eta_1 V_{CNT} E_{r11} + (1 - V_{CNT}) E_{11}^{m}, \tag{1}$$

$$\frac{\eta_2}{E_{22}}=\frac{V_{CNT}}{E_{r22}}+\frac{(1-V_{CNT})}{E_{22}^{m}}, \tag{2}$$

$$\frac{\eta_3}{G_{12}}=\frac{V_{CNT}}{G_{r12}}+\frac{(1-V_{CNT})}{G_{12}^{m}}, \tag{3}$$

where E_{r11}, E_{r22} and G_{r12} represent Young's and shear moduli of CNTs, respectively. Also, E_m and G_m are the mechanical properties of the matrix material, and V_{CNT} indicates the volume fraction of CNTs. In addition, η_i (i = 1, 2, 3) denotes the CNT efficiency parameters. Here, CNTs are considered to be distributed uniformly (UD) or functionally graded (FG) through the thickness direction of the composite curved microbeam. Four different CNTs distribution types can be defined as below

$$UD:\quad V_{CNT}=V_{CNT}^{*}, \tag{4}$$

$$FGA:\ V_{CNT}(z)=\left(1-\frac{2z}{h}\right)V_{CNT}^{*}, \tag{5}$$

$$FGO:\ V_{CNT}(z)=2\left(1-\frac{2|z|}{h}\right)V_{CNT}^{*}, \tag{6}$$

$$FGX:\ V_{CNT}(z)=2\left(\frac{2|z|}{h}\right)V_{CNT}^{*}, \tag{7}$$

in which

$$V_{CNT}^{*}=\frac{w_{CNT}}{w_{CNT}+(\rho_{CNT}/\rho_m)-(\rho_{CNT}/\rho_m)w_{CNT}}, \tag{8}$$

in which w_{CNT} denote the mass fraction of CNTs; ρ_m and ρ_{CNT} are the mass densities of matrix and CNTs, respectively. Also, the effective thermal expansion coefficients and mass density of the CNTs-reinforced composite beam can be calculated based on the extended rule of mixture as below

$$\begin{aligned}\alpha_{xx}^{(c)}&=V_{CNT}\alpha_{r11}+\left(1-V_{CNT}\right)\alpha_{m},\\ \alpha_{zz}^{(c)}&=\left(1+\nu_{r12}\right)V_{CNT}\alpha_{r22}\\ &+\left(1+\nu_m\right)\left(1-V_{CNT}\right)\alpha_m-\nu_{12}\alpha_{11},\end{aligned} \tag{9}$$

$$\rho^{(c)}=V_{CNT}\rho_r+\left(1-V_{CNT}\right)\rho_m, \tag{10}$$

where α_{r11} and α_{r22} represent the thermal expansion coefficients of CNT in the longitudinal and transverse directions, respectively. In addition, ρ_m and ρ_r indicate the mass densities of matrix and CNT, respectively. It should be noted that the Poisson's ratio is assumed to be constant in direction of the thickness.

3.2 Timoshenko beam theory

Based on Timoshenko beam theory, the displacement field at any point of the microbeam can be considered as follows (Liu and Reddy 2011)

$$\begin{aligned}u_x(x,z,t)&=u(x,t)-z\,\varphi(x,t),\\ u_z(x,z,t)&=w(x,t),\end{aligned} \tag{11}$$

in which $u(x, t)$ and $w(x, t)$ are the displacement components of the mid-plane along x and z directions, $\varphi(x, t)$ is the total bending rotation of the microbeam cross section and t denotes time. The strain tensor components can be calculated using following relation

$$\varepsilon_{ij}=\frac{1}{2}(u_{i,j}+u_{j,i}), \tag{12}$$

Substituting Eq. (11) into Eq. (12) we have

$$\varepsilon_{xx}=\frac{\partial u}{\partial x}+\frac{w}{R}+z\,\frac{\partial \varphi}{\partial x}, \tag{13a}$$

$$\varepsilon_{xz}=\frac{1}{2}\left(\frac{\partial w}{\partial x}-\frac{u}{R}+\left(1-\frac{z}{R}\right)\varphi\right), \tag{13b}$$

3.3 Strain gradient theory

The strain gradient theory is proposed by Lam (2003). This theory captures the size effect by considering three independent material length scale parameters and defines the potential energy as a function of the symmetric strain tensor, the dilatation gradient vector, the deviatoric stretch gradient tensor and the symmetric rotation gradient tensor. So, the potential strain energy of the microbeam can be expressed as below (Lam *et al*. 2003)

$$U=\frac{1}{2}\int_V\left(\sigma_{ij}\varepsilon_{ij}+p_i\gamma_i+\tau_{ijk}^{(1)}\eta_{ijk}^{(1)}+m_{ij}^{s}\chi_{ij}^{s}\right)dV, \tag{14}$$

where γ_i, $\eta_{ijk}^{(1)}$ and χ_{ij} indicate the dilatation gradient vector, the deviatoric stretch gradient and the symmetric rotation gradient tensors, respectively and may be defined by the following relations

$$\gamma_i=\varepsilon_{mm,i}, \tag{15a}$$

$$\begin{aligned}\eta_{ijk}&=\frac{1}{3}(\varepsilon_{jk,i}+\varepsilon_{ki,j}+\varepsilon_{ij,k})-\frac{1}{15}\delta_{ij}(\varepsilon_{mm,k}+2\varepsilon_{mk,m})\\ &-\frac{1}{15}\left[\delta_{jk}(\varepsilon_{mm,i}+2\varepsilon_{mi,m})+\delta_{ki}(\varepsilon_{mm,j}+2\varepsilon_{mj,m})\right],\end{aligned} \tag{15b}$$

$$\chi_{ij}^{s}=\frac{1}{2}(\theta_{i,j}+\theta_{j,i}), \tag{15c}$$

in which u_i and δ_{ij} denote the displacement vector and the knocker delta, respectively. Also, the rotation vector (θ_i) can be defined as follows

$$\theta_i=\left(\frac{1}{2}curl(u)\right)_i. \tag{16}$$

The total potential strain energy of the microbeam based on Timoshenko beam theory can be rewritten as

$$\begin{aligned} U = \frac{1}{2}\int_V \big(&\sigma_{xx}\varepsilon_{xx} + 2\tau_{xz}\varepsilon_{xz} + p_x\gamma_x + p_z\gamma_z \\ &+\tau^{(1)}_{xxx}\eta^{(1)}_{xxx} + \tau^{(1)}_{zzz}\eta^{(1)}_{zzz} + 3\tau^{(1)}_{xxz}\eta^{(1)}_{xxz} + 3\tau^{(1)}_{yyx}\eta^{(1)}_{yyx} \\ &+3\tau^{(1)}_{yyz}\eta^{(1)}_{yyz} + 3\tau^{(1)}_{zzx}\eta^{(1)}_{zzx} + 2m^s_{xy}\chi^s_{xy} + 2m^s_{yz}\chi^s_{yz}\big)dV \end{aligned} \tag{17}$$

Using Eqs. (11)-(13b), the dilatation gradient vector, the deviatoric stretch gradient and the symmetric rotation gradient tensors can be simplified as

$$\gamma_x = \varepsilon_{xx,x} = \frac{\partial^2 u}{\partial x^2} + \frac{1}{R}\frac{\partial w}{\partial x} + z\frac{\partial^2 \varphi}{\partial x^2}, \tag{18a}$$

$$\gamma_z = \varepsilon_{xx,z} = \frac{\partial \varphi}{\partial x}, \tag{18b}$$

$$\begin{aligned} \theta_y &= \frac{1}{2}\left(\frac{\partial u_x}{\partial z} - \frac{\partial u_z}{\partial x} + \frac{u_x}{R}\right) \\ &= \frac{1}{2}\left(\varphi_y - \frac{\partial w}{\partial x} + \frac{u}{R} + \frac{z}{R}\varphi\right), \end{aligned} \tag{19}$$

$$\eta^{(1)}_{xxx} = \frac{2}{5}\left(\frac{\partial^2 u}{\partial x^2} + \frac{1}{R}\frac{\partial w}{\partial x} + z\frac{\partial^2 \varphi}{\partial x^2} + \frac{1}{2R}\varphi\right), \tag{20a}$$

$$\eta^{(1)}_{zzz} = -\frac{1}{5}\left(\frac{\partial \varphi}{\partial x} + \frac{\partial^2 w}{\partial x^2} - \frac{1}{R}\frac{\partial u}{\partial x} + \left(1 - \frac{z}{R}\right)\frac{\partial \varphi}{\partial x}\right), \tag{20b}$$

$$\begin{aligned} &\eta^{(1)}_{xxz} = \eta^{(1)}_{xzx} = \eta^{(1)}_{zxx} = \\ &\frac{4}{15}\left(\frac{\partial \varphi}{\partial x} + \frac{\partial^2 w}{\partial x^2} - \frac{1}{R}\frac{\partial u}{\partial x} + \left(1 - \frac{z}{R}\right)\frac{\partial \varphi}{\partial x}\right), \end{aligned} \tag{20c}$$

$$\begin{aligned} &\eta^{(1)}_{yyx} = \eta^{(1)}_{yxy} = \eta^{(1)}_{xyy} = \\ &-\frac{1}{5}\left(\frac{\partial^2 u}{\partial x^2} + \frac{1}{R}\frac{\partial w}{\partial x} + z\frac{\partial^2 \varphi}{\partial x^2}\right) + \frac{1}{15R}\varphi, \end{aligned} \tag{20d}$$

$$\begin{aligned} &\eta^{(1)}_{yyz} = \eta^{(1)}_{yzy} = \eta^{(1)}_{zyy} = \\ &-\frac{1}{15}\left(\frac{\partial \varphi}{\partial x} + \frac{\partial^2 w}{\partial x^2} - \frac{1}{R}\frac{\partial u}{\partial x} + \left(1 - \frac{z}{R}\right)\frac{\partial \varphi}{\partial x}\right), \end{aligned} \tag{20e}$$

$$\eta^{(1)}_{zzz} = -\frac{1}{5}\left(\frac{\partial \varphi}{\partial x} + \frac{\partial^2 w}{\partial x^2} - \frac{1}{R}\frac{\partial u}{\partial x} + \left(1 - \frac{z}{R}\right)\frac{\partial \varphi}{\partial x}\right), \tag{20f}$$

$$\begin{aligned} &\eta^{(1)}_{zzx} = \eta^{(1)}_{zxz} = \eta^{(1)}_{xzz} = \\ &-\frac{1}{5}\left(\frac{\partial^2 u}{\partial x^2} + \frac{1}{R}\frac{\partial w}{\partial x} + z\frac{\partial^2 \varphi}{\partial x^2}\right) - \frac{4}{15}\varphi, \end{aligned} \tag{21a}$$

$$\chi^s_{yz} = \frac{1}{2}\left(\frac{\partial \theta_z}{\partial y} + \frac{\partial \theta_y}{\partial z}\right) = \frac{1}{4R}\varphi. \tag{21b}$$

Also, the classical stress tensor, σ_{ij}, the higher-order stresses, p_i, $\tau^{(1)}_{ijk}$ and m_{ij} can be defined as

$$\sigma_{ij} = \lambda tr\varepsilon\delta_{ij} + 2\mu\varepsilon_{ij}, \tag{22a}$$

$$p_i = 2\mu l_0^2 \gamma_i, \tag{22b}$$

$$\tau^1_{ijk} = 2\mu l_1^2 \eta^1_{ijk}, \tag{22c}$$

$$m^s_{ij} = 2\mu l_2^2 \chi^s_{ij}, \tag{22d}$$

where (l_0, l_1, l_2) denote the independent material length scale parameters, λ and μ are the bulk and shear modulus, respectively. Substituting Eqs. (13a), (13b) and (18a)-(21b) into (22a)-(22d) we have

$$\sigma_{xx} = Q_{11}(z)\varepsilon_{xx} = Q_{11}(z)\left(\frac{\partial u}{\partial x} + \frac{w}{R} + z\frac{\partial \varphi}{\partial x}\right), \tag{23a}$$

$$\begin{aligned} \tau_{xz} &= Q_{22}(z)\varepsilon_{xz} = \\ &Q_{22}(z)\left(\left(\frac{\partial w}{\partial x} - \frac{u}{R} + \left(1 - \frac{z}{R}\right)\varphi\right)\right), \end{aligned} \tag{23b}$$

$$p_x = 2\mu l_0^2 \gamma_x = 2\mu l_0^2\left(\frac{\partial^2 u}{\partial x^2} + \frac{1}{R}\frac{\partial w}{\partial x} + z\frac{\partial^2 \varphi}{\partial x^2}\right), \tag{24a}$$

$$p_z = 2\mu l_0^2 \gamma_z = 2\mu l_0^2 \frac{\partial \varphi}{\partial x}, \tag{24b}$$

$$\tau^{(1)}_{xxx} = \frac{2}{5}\mu l_1^2\left(\frac{\partial^2 u}{\partial x^2} + \frac{1}{R}\frac{\partial w}{\partial x} + z\frac{\partial^2 \varphi}{\partial x^2} + \frac{1}{2R}\varphi\right), \tag{25a}$$

$$\tau^{(1)}_{zzz} = -\frac{2}{5}\mu l_1^2\left(\frac{\partial \varphi}{\partial x} + \frac{\partial^2 w}{\partial x^2} - \frac{1}{R}\frac{\partial u}{\partial x} + \left(1 - \frac{z}{R}\right)\frac{\partial \varphi}{\partial x}\right), \tag{25b}$$

$$\tau^{(1)}_{xxz} = \frac{8}{15}\mu l_1^2\left(\frac{\partial \varphi}{\partial x} + \frac{\partial^2 w}{\partial x^2} - \frac{1}{R}\frac{\partial u}{\partial x} + \left(1 - \frac{z}{R}\right)\frac{\partial \varphi}{\partial x}\right), \tag{25c}$$

$$\tau^{(1)}_{yyx} = -\frac{2}{5}\mu l_1^2\left(\frac{\partial^2 u}{\partial x^2} + \frac{1}{R}\frac{\partial w}{\partial x} + z\frac{\partial^2 \varphi}{\partial x^2}\right) + \frac{2}{15R}\mu l_1^2\varphi, \tag{25d}$$

$$\tau^{(1)}_{yyz} = -\frac{2}{15}\mu l_1^2\left(\frac{\partial \varphi}{\partial x} + \frac{\partial^2 w}{\partial x^2} - \frac{1}{R}\frac{\partial u}{\partial x} + \left(1 - \frac{z}{R}\right)\frac{\partial \varphi}{\partial x}\right), \tag{25e}$$

$$\tau^{(1)}_{zzx} = -\frac{2}{5}\mu l_1^2\left(\frac{\partial^2 u}{\partial x^2} + \frac{1}{R}\frac{\partial w}{\partial x} + z\frac{\partial^2 \varphi}{\partial x^2}\right) - \frac{8}{15}\mu l_1^2\varphi, \tag{25f}$$

$$m^s_{xy} = \frac{\mu l_2^2}{2}\left(\frac{\partial \varphi}{\partial x} - \frac{\partial^2 w}{\partial x^2} + \frac{1}{R}\frac{\partial u}{\partial x} + \frac{z}{R}\frac{\partial \varphi}{\partial x}\right), \tag{26a}$$

$$m^s_{yz} = \frac{\mu l_2^2}{2R}\varphi, \tag{26b}$$

where

$$Q_{11}(z)=\frac{E(z)}{1-\nu_{12}(z)\nu_{21}(z)}\left(1+g\frac{\partial}{\partial t}\right), \tag{27a}$$

$$Q_{22}(z)=G_{12}(z)\left(1+g\frac{\partial}{\partial t}\right), \tag{27b}$$

in which g represents the structural damping constant.

3.4 Hamilton's principle

In this work, the governing equations of the microbeam are derived using Hamilton's principle which can be defined as follows

$$\int_0^t\left(\delta U-\left(\delta K+\delta W\right)\right)dt=0. \tag{28}$$

In which U represent the total potential strain energy; K and W are the kinetic energy and the work done by the external forces, respectively. In addition, δ denote the vibration operator.

The kinetic energy of the microbeam can be calculated as

$$K=\frac{\rho}{2}\int_0^L\int_A\left(\left(\frac{\partial u_x}{\partial t}\right)^2+\left(\frac{\partial u_z}{\partial t}\right)^2\right)dA\,dx, \tag{29}$$

in which ρ is the mass density of the nanocomposite microbeam. Also, the work done by surrounding elastic medium and axial magnetic field can be obtained as follows (Kolahchi *et al*. 2016b, Shen and Zhang 2011)

$$W=\frac{1}{2}\int_0^L\begin{pmatrix}-k_w w-c_d\dot{w}+k_g\dfrac{\partial^2 w}{\partial x^2}\\ +\eta A H_x^2\dfrac{\partial^2 w}{\partial x^2}\end{pmatrix}w\,dx, \tag{30}$$

where k_w and k_g denote the spring constant of the Winkler type and the shear constant of the Pasternak type, respectively. Also, c_d represents the damper constant of foundation; η is the magnetic field permeability and $H_x$denotes the axial magnetic field. Furthermore, the foundation stiffness k_w for the soft medium may be considered as (Shen and Zhang 2011)

$$k_w=\frac{E_0}{4L(1-\nu_0^2)(2-c_1)^2}\left[5-\left(2\gamma_1^2+6\gamma_1+5\right)\exp\left(-2\gamma_1\right)\right], \tag{31a}$$

in which

$$c_1=\left(\gamma_1+2\right)\exp\left(-\gamma_1\right), \tag{31b}$$

$$\gamma_1=\frac{H_s}{L}, \tag{31c}$$

$$E_0=\frac{E_s}{\left(1-\nu_s^2\right)}, \tag{31d}$$

$$\nu_0=\frac{\nu_s}{\left(1-\nu_s\right)}, \tag{31e}$$

in which E_s, ν_s, H_s denote Young's modulus, Poisson's ratio and depth of the foundation, respectively. In this work, it is assumed that E_s is temperature-dependent while ν_s is a constant.

3.5 Derivation of governing equations

Substituting Eqs. (17), (29) and (30) into Eq. (28), the motion equations of the microbeam can be obtained as below

$$\begin{aligned}&\frac{\partial N_x}{\partial x}+\frac{Q_{xz}}{R}-\frac{2}{5}\frac{\partial^2 T_{xxx}}{\partial x^2}+\frac{1}{5R}\frac{\partial T_{zzz}}{\partial x}-\frac{4}{5R}\frac{\partial T_{xxz}}{\partial x}\\&+\frac{3}{5}\frac{\partial^2 T_{yyx}}{\partial x^2}+\frac{1}{5R}\frac{\partial T_{yyz}}{\partial x}+\frac{3}{5}\frac{\partial^2 T_{zzx}}{\partial x^2}-\frac{\partial^2 P_x}{\partial x^2}\\&+\frac{1}{2R}\frac{\partial Y_{xy}}{\partial x}=I_1\frac{\partial^2 u}{\partial t^2}-I_2\frac{\partial^2\varphi}{\partial t^2},\end{aligned} \tag{32}$$

$$\begin{aligned}&-\frac{N_x}{R}+\frac{\partial Q_{xz}}{\partial x}+\frac{2}{5R}\frac{\partial T_{xxx}}{\partial x}+\frac{1}{5}\frac{\partial^2 T_{zzz}}{\partial x^2}-\frac{4}{5}\frac{\partial^2 T_{xxz}}{\partial x^2}\\&-\frac{3}{5R}\frac{\partial T_{yyx}}{\partial x}+\frac{1}{5}\frac{\partial^2 T_{yyz}}{\partial x^2}-\frac{3}{5R}\frac{\partial T_{zzx}}{\partial x}+\frac{1}{R}\frac{\partial P_x}{\partial x}\\&+\frac{1}{2}\frac{\partial^2 Y_{xy}}{\partial x^2}-k_w w-c_d\dot{w}+k_g\frac{\partial^2 w}{\partial x^2}\\&+\eta A H_x^2\frac{\partial^2 w}{\partial x^2}=I_1\frac{\partial^2 w}{\partial t^2},\end{aligned} \tag{33}$$

$$\begin{aligned}&\frac{\partial M_x}{\partial x}-Q_{xz}+\frac{1}{R}P_{xz}-\frac{2}{5}\frac{\partial^2 M_{xxx}}{\partial x^2}-\frac{1}{5R}T_{xxx}-\frac{2}{5}\frac{\partial T_{zzz}}{\partial x}\\&+\frac{1}{5R}\frac{\partial M_{zzz}}{\partial x}+\frac{8}{5}\frac{\partial T_{xxz}}{\partial x}-\frac{4}{5R}\frac{\partial M_{xxz}}{\partial x}+\frac{3}{5}\frac{\partial^2 M_{yyx}}{\partial x^2}\\&-\frac{1}{5R}T_{yyx}-\frac{2}{5}\frac{\partial T_{yyz}}{\partial x}+\frac{1}{5R}\frac{\partial M_{yyz}}{\partial x}+\frac{4}{5R}T_{zzx}\\&+\frac{3}{5}\frac{\partial^2 M_{zzx}}{\partial x^2}-\frac{\partial^2 S_x}{\partial x^2}+\frac{\partial P_z}{\partial x}+\frac{1}{2}\frac{\partial Y_{xy}}{\partial x}+\frac{1}{2R}\frac{\partial X_{xy}}{\partial x}\\&-\frac{1}{2R}Y_{yz}=I_3\frac{\partial^2\varphi}{\partial t^2}-I_2\frac{\partial^2 u}{\partial t^2},\end{aligned} \tag{34}$$

where the stress resultants can be expressed as

$$\begin{aligned}N_x&=\int_s\sigma_{xx}dA=A_{11}\frac{\partial u}{\partial x}+A_{11}\frac{w}{R}+B_{11}\frac{\partial\varphi}{\partial x}\\&+g\left(A_{11}\frac{\partial^2 u}{\partial t\,\partial x}+A_{11}\frac{1}{R}\frac{\partial w}{\partial t}+B_{11}\frac{\partial^2\varphi}{\partial t\,\partial x}\right),\end{aligned} \tag{35a}$$

$$\begin{aligned}M_x&=\int_s\sigma_{xx}z\,dA=B_{11}\frac{\partial u}{\partial x}+B_{11}\frac{w}{R}+D_{11}\frac{\partial\varphi}{\partial x}\\&+g\left(B_{11}\frac{\partial^2 u}{\partial t\,\partial x}+B_{11}\frac{1}{R}\frac{\partial w}{\partial t}+D_{11}\frac{\partial^2\varphi}{\partial t\,\partial x}\right),\end{aligned} \tag{35b}$$

$$Q_{xz}=\int_s\tau_{xz}dA=k_s\left(A_{22}\frac{\partial w}{\partial x}-A_{22}\frac{u}{R}+\left(A_{22}-\frac{B_{22}}{R}\right)\varphi\right. \tag{36a}$$

$$+\mathrm{g}\left(A_{22}\frac{\partial^2 w}{\partial t\,\partial x}-A_{22}\frac{1}{R}\frac{\partial u}{\partial t}+\left(A_{22}-\frac{B_{22}}{R}\right)\frac{\partial\varphi}{\partial t}\right)\Bigg), \quad (36a)$$

$$P_{xz}=\int_s \tau_{xz}\,z\,dA=B_{22}\frac{\partial w}{\partial x}-B_{22}\frac{u}{R}+\left(B_{22}-\frac{D_{22}}{R}\right)\varphi +\mathrm{g}\left(B_{22}\frac{\partial^2 w}{\partial t\,\partial x}-B_{22}\frac{1}{R}\frac{\partial u}{\partial t}+\left(B_{22}-\frac{D_{22}}{R}\right)\frac{\partial\varphi}{\partial t}\right), \quad (36b)$$

$$P_x=\int_s p_x\,dA=2l_0^2\left(A_{22}\frac{\partial^2 u}{\partial x^2}+A_{22}\frac{1}{R}\frac{\partial w}{\partial x}+B_{22}\frac{\partial^2\varphi}{\partial x^2}+\mathrm{g}\left(A_{22}\frac{\partial^3 u}{\partial t\,\partial x^2}+A_{22}\frac{1}{R}\frac{\partial^2 w}{\partial t\,\partial x}+B_{22}\frac{\partial^3\varphi}{\partial t\,\partial x^2}\right)\right), \quad (37a)$$

$$S_x=\int_s p_x\,z\,dA=2l_0^2\left(B_{22}\frac{\partial^2 u}{\partial x^2}+B_{22}\frac{1}{R}\frac{\partial w}{\partial x}+D_{22}\frac{\partial^2\varphi}{\partial x^2}+\mathrm{g}\left(B_{22}\frac{\partial^3 u}{\partial t\,\partial x^2}+B_{22}\frac{1}{R}\frac{\partial^2 w}{\partial t\,\partial x}+D_{22}\frac{\partial^3\varphi}{\partial t\,\partial x^2}\right)\right), \quad (37b)$$

$$P_z=\int_s p_z\,dA=2l_0^2\left(A_{22}\frac{\partial\varphi}{\partial x}+\mathrm{g}\,A_{22}\frac{\partial^2\varphi}{\partial t\,\partial x}\right), \quad (37c)$$

$$Y_{xy}=\int_s m_{xy}\,dA=\frac{l_2^2}{2}\left(A_{22}\frac{\partial\varphi}{\partial x}-A_{22}\frac{\partial^2 w}{\partial x^2}+A_{22}\frac{1}{R}\frac{\partial u}{\partial x}+B_{22}\frac{1}{R}\frac{\partial\varphi}{\partial x}+\mathrm{g}\left(A_{22}\frac{\partial^2\varphi}{\partial t\,\partial x}-A_{22}\frac{\partial^3 w}{\partial t\,\partial x^2}+A_{22}\frac{1}{R}\frac{\partial^2 u}{\partial t\,\partial x}+B_{22}\frac{1}{R}\frac{\partial^2\varphi}{\partial t\,\partial x}\right)\right), \quad (38a)$$

$$X_{xy}=\int_s m_{xy}\,z\,dA=\frac{l_2^2}{2}\left(B_{22}\frac{\partial\varphi}{\partial x}-B_{22}\frac{\partial^2 w}{\partial x^2}+B_{22}\frac{1}{R}\frac{\partial u}{\partial x}+D_{22}\frac{1}{R}\frac{\partial\varphi}{\partial x}+\mathrm{g}\left(B_{22}\frac{\partial^2\varphi}{\partial t\,\partial x}-B_{22}\frac{\partial^3 w}{\partial t\,\partial x^2}+B_{22}\frac{1}{R}\frac{\partial^2 u}{\partial t\,\partial x}+D_{22}\frac{1}{R}\frac{\partial^2\varphi}{\partial t\,\partial x}\right)\right), \quad (38b)$$

$$Y_{yz}=\int_s m_{yz}\,dA=\frac{l_2^2}{2R}\left(A_{22}\varphi+gA_{22}\frac{\partial\varphi}{\partial t}\right), \quad (38c)$$

$$T_{xxx}=\int_s \tau_{xxx}^{(1)}\,dA=\frac{4}{5}l_1^2\left(A_{22}\frac{\partial^2 u}{\partial x^2}+A_{22}\frac{1}{R}\frac{\partial w}{\partial x}+B_{22}\frac{\partial^2\varphi}{\partial x^2}+A_{22}\frac{1}{2R}\varphi+\mathrm{g}\left(A_{22}\frac{\partial^3 u}{\partial t\,\partial x^2}+A_{22}\frac{1}{R}\frac{\partial^2 w}{\partial t\,\partial x}+B_{22}\frac{\partial^3\varphi}{\partial t\,\partial x^2}+A_{22}\frac{1}{2R}\frac{\partial\varphi}{\partial t}\right), \quad (39a)$$

$$M_{xxx}=\int_s \tau_{xxx}^{(1)}\,z\,dA=\frac{4}{5}l_1^2\left(B_{22}\frac{\partial^2 u}{\partial x^2}+B_{22}\frac{1}{R}\frac{\partial w}{\partial x}+D_{22}\frac{\partial^2\varphi}{\partial x^2}+B_{22}\frac{1}{2R}\varphi_y+\mathrm{g}\left(B_{22}\frac{\partial^2 u}{\partial t\,\partial x^2}+B_{22}\frac{1}{R}\frac{\partial^2 w}{\partial t\,\partial x}+D_{22}\frac{\partial^3\varphi}{\partial t\,\partial x^2}+B_{22}\frac{1}{2R}\frac{\partial\varphi}{\partial t}\right)\right), \quad (39b)$$

$$T_{zzz}=\int_s \tau_{zzz}^{(1)}\,dA=-\frac{2}{5}l_1^2\left(A_{22}\frac{\partial\varphi}{\partial x}+A_{22}\frac{\partial^2 w}{\partial x^2}-A_{22}\frac{1}{R}\frac{\partial u}{\partial x}+\left(A_{22}-\frac{B_{22}}{R}\right)+\mathrm{g}\left(A_{22}\frac{\partial^2\varphi}{\partial t\,\partial x}+A_{22}\frac{\partial^3 w}{\partial t\,\partial x^2}-A_{22}\frac{1}{R}\frac{\partial^2 u}{\partial t\,\partial x}+\left(A_{22}-\frac{B_{22}}{R}\right)\frac{\partial^2\varphi}{\partial t\,\partial x}\right)\right), \quad (39c)$$

$$M_{zzz}=\int_s \tau_{zzz}^{(1)}\,z\,dA=-\frac{2}{5}l_1^2\left(B_{22}\frac{\partial\varphi}{\partial x}+B_{22}\frac{\partial^2 w}{\partial x^2}-B_{22}\frac{1}{R}\frac{\partial u}{\partial x}+\left(B_{22}-\frac{D_{22}}{R}\right)\frac{\partial\varphi}{\partial x}+\mathrm{g}\left(B_{22}\frac{\partial^2\varphi}{\partial t\,\partial x}+B_{22}\frac{\partial^3 w}{\partial t\,\partial x^2}-B_{22}\frac{1}{R}\frac{\partial^2 u}{\partial t\,\partial x}+\left(B_{22}-\frac{D_{22}}{R}\right)\frac{\partial^2\varphi}{\partial t\,\partial x}\right)\right) \quad (39d)$$

$$T_{xxz}=\int_s \tau_{xxz}^{(1)}\,dA=\frac{8}{15}l_1^2\left(A_{22}\frac{\partial\varphi}{\partial x}+A_{22}\frac{\partial^2 w}{\partial x^2}-A_{22}\frac{1}{R}\frac{\partial u}{\partial x}+\left(A_{22}-\frac{B_{22}}{R}\right)\frac{\partial\varphi}{\partial x}+\mathrm{g}\left(A_{22}\frac{\partial^2\varphi}{\partial t\,\partial x}+A_{22}\frac{\partial^3 w}{\partial t\,\partial x^2}-A_{22}\frac{1}{R}\frac{\partial^2 u}{\partial t\,\partial x}+\left(A_{22}-\frac{B_{22}}{R}\right)\frac{\partial^2\varphi}{\partial t\,\partial x}\right)\right), \quad (39e)$$

$$M_{xxz}=\int_s \tau_{xxz}^{(1)}\,z\,dA=\frac{8}{15}l_1^2\left(B_{22}\frac{\partial\varphi}{\partial x}+B_{22}\frac{\partial^2 w}{\partial x^2}\frac{\partial u}{\partial x}-B_{22}\frac{1}{R}+\left(B_{22}-\frac{D_{22}}{R}\right)\frac{\partial\varphi}{\partial x}+\mathrm{g}\left(B_{22}\frac{\partial^2\varphi}{\partial t\,\partial x}+B_{22}\frac{\partial^3 w}{\partial t\,\partial x^2}-B_{22}\frac{1}{R}\frac{\partial^2 u}{\partial t\,\partial x}+\left(B_{22}-\frac{D_{22}}{R}\right)\frac{\partial^2\varphi}{\partial t\,\partial x}\right)\right), \quad (39f)$$

$$T_{yyx}=\int_s \tau_{yyx}^{(1)}\,dA=-\frac{2}{5}l_1^2\left(A_{22}\frac{\partial^2 u}{\partial x^2}+A_{22}\frac{1}{R}\frac{\partial w}{\partial x}+B_{22}\frac{\partial^2\varphi}{\partial x^2}+\frac{2}{15R}l_1^2A_{22}\varphi+\mathrm{g}\left(A_{22}\frac{\partial^3 u}{\partial t\,\partial x^2}+A_{22}\frac{1}{R}\frac{\partial^2 w}{\partial t\,\partial x}+B_{22}\frac{\partial^3\varphi}{\partial t\,\partial x^2}+\frac{2}{15R}l_1^2A_{22}\frac{\partial\varphi}{\partial t}\right)\right), \quad (39g)$$

$$M_{yyx}=\int_s \tau_{yyx}^{(1)}\,z\,dA=-\frac{2}{5}l_1^2\left(B_{22}\frac{\partial^2 u}{\partial x^2}+B_{22}\frac{1}{R}\frac{\partial w}{\partial x}+D_{22}\frac{\partial^2\varphi}{\partial x^2}+\mathrm{g}\left(B_{22}\frac{\partial^3 u}{\partial t\,\partial x^2}+B_{22}\frac{1}{R}\frac{\partial^2 w}{\partial t\,\partial x}+D_{22}\frac{\partial^3\varphi}{\partial t\,\partial x^2}\right)\right)+\frac{2}{15R}l_1^2\left(B_{22}\varphi+gB_{22}\frac{\partial\varphi}{\partial t}\right), \quad (39h)$$

$$T_{yyz}=\int_s \tau_{yyz}^{(1)}\,dA=-\frac{2}{15}l_1^2\left(A_{22}\frac{\partial\varphi}{\partial x}+A_{22}\frac{\partial^2 w}{\partial x^2}-A_{22}\frac{1}{R}\frac{\partial u}{\partial x}+\left(A_{22}-\frac{B_{22}}{R}\right)\frac{\partial\varphi}{\partial x}+\mathrm{g}\left(A_{22}\frac{\partial^2\varphi}{\partial t\,\partial x}+A_{22}\frac{\partial^3 w}{\partial t\,\partial x^2}-A_{22}\frac{1}{R}\frac{\partial^2 u}{\partial t\,\partial x}+\left(A_{22}-\frac{B_{22}}{R}\right)\frac{\partial^2\varphi}{\partial t\,\partial x}\right)\right), \quad (39i)$$

$$M_{yyz}=\int_s \tau_{yyz}^{(1)}\,z\,dA=-\frac{2}{15}l_1^2\left(B_{22}\frac{\partial\varphi}{\partial x}+B_{22}\frac{\partial^2 w}{\partial x^2}-B_{22}\frac{1}{R}\frac{\partial u}{\partial x}+\left(B_{22}-\frac{D_{22}}{R}\right)\frac{\partial\varphi}{\partial x}+\mathrm{g}\left(B_{22}\frac{\partial^2\varphi}{\partial t\,\partial x}+B_{22}\frac{\partial^3 w}{\partial t\,\partial x^2}-B_{22}\frac{1}{R}\frac{\partial^2 u}{\partial t\,\partial x}+\left(B_{22}-\frac{D_{22}}{R}\right)\frac{\partial^2\varphi}{\partial t\,\partial x}\right)\right), \quad (39j)$$

$$T_{zzx}=\int_s \tau_{zzx}^{(1)}\,dA=-\frac{2}{5}l_1^2\left(A_{22}\frac{\partial^2 u}{\partial x^2}+A_{22}\frac{1}{R}\frac{\partial w}{\partial x}+B_{22}\frac{\partial^2\varphi}{\partial x^2}\right. \quad (39k)$$

$$+\mathrm{g}\left(A_{22}\frac{\partial^3 u}{\partial t\partial x^2}+A_{22}\frac{1}{R}\frac{\partial^2 w}{\partial t\partial x}+B_{22}\frac{\partial^3 \varphi}{\partial t\partial x^2}\right)\Bigg)\cdot$$
$$-\frac{8}{15}l_1^2\left(A_{22}\varphi_y+gA_{22}\frac{\partial\varphi}{\partial t}\right), \tag{39k}$$

$$M_{zzx}=\int_s \tau_{zzx}^{(1)} z dA=-\frac{2}{5}l_1^2\left(B_{22}\frac{\partial^2 u}{\partial x^2}+B_{22}\frac{1}{R}\frac{\partial w}{\partial x}+D_{22}\frac{\partial^2 \varphi}{\partial x^2}\right.\cdot$$
$$+\mathrm{g}\left(B_{22}\frac{\partial^3 u}{\partial t\partial x^2}+B_{22}\frac{1}{R}\frac{\partial^2 w}{\partial t\partial x}+D_{22}\frac{\partial^3 \varphi}{\partial t\partial x^2}\right)\Bigg) \tag{39l}$$
$$-\frac{8}{15}l_1^2\left(B_{22}\varphi+gB_{22}\frac{\partial\varphi}{\partial t}\right),$$

Substituting Eq. (35a)-(39l) into Eqs. (32)-(34), the governing equations can be obtained as below

$$A_{11}\frac{\partial^2 u}{\partial x^2}+\frac{A_{11}}{R}\frac{\partial w}{\partial x}+B_{11}\frac{\partial^2\varphi}{\partial x^2}+\frac{K_s}{R}\left(\frac{A_{22}}{R}\frac{\partial w}{\partial x}-\frac{A_{22}}{R}u+A_{22}\varphi-\frac{B_{22}}{R}\varphi\right)-\frac{8}{25}l_1^2\left(A_{22}\frac{\partial^4 u}{\partial x^4}\right.$$
$$+\frac{A_{22}}{R}\frac{\partial^3 w}{\partial x^3}+\frac{1}{2}\frac{A_{22}}{R}\frac{\partial^2\varphi}{\partial x^2}+B_{22}\frac{\partial^4\varphi}{\partial x^4}\Big)-\frac{8}{15}\frac{l_1^2}{R}\left(2A_{22}\frac{\partial^2\varphi}{\partial x^2}+A_{22}\frac{\partial^3 w}{\partial x^3}-\frac{A_{22}}{R}\frac{\partial^2 u}{\partial x^2}-\frac{B_{22}}{R}\frac{\partial^2\varphi}{\partial x^2}\right)$$
$$-\frac{12}{25}l_1^2\left(A_{22}\frac{\partial^4 u}{\partial x^4}+\frac{A_{22}}{R}\frac{\partial^3 w}{\partial x^3}+B_{22}\frac{\partial^4\varphi}{\partial x^4}\right)-\frac{6}{25}\frac{l_1^2A_{22}}{R}\frac{\partial^2\varphi}{\partial x^2}-2l_0^2\left(A_{22}\frac{\partial^4 u}{\partial x^4}+\frac{A_{22}}{R}\frac{\partial^3 w}{\partial x^3}\right.$$
$$+B_{22}\frac{\partial^4\varphi}{\partial x^4}\Big)+\frac{1}{4}\frac{l_2^2}{R}\left(A_{22}\frac{\partial^2\varphi}{\partial x^2}-A_{22}\frac{\partial^3 w}{\partial x^3}+\frac{A_{22}}{R}\frac{\partial^2 u}{\partial x^2}+\frac{B_{22}}{R}\frac{\partial^2\varphi}{\partial x^2}\right)$$
$$+g\begin{pmatrix}A_{11}\frac{\partial^3 u}{\partial t\partial x^2}+\frac{A_{11}}{R}\frac{\partial^2 w}{\partial t\partial x}+B_{11}\frac{\partial^3\varphi}{\partial t\partial x^2}+\frac{K_s}{R}\left(\frac{A_{22}}{R}\frac{\partial^2 w}{\partial t\partial x}-\frac{A_{22}}{R}\frac{\partial u}{\partial t}\right.\\+A_{22}\frac{\partial\varphi}{\partial t}-\frac{B_{22}}{R}\frac{\partial\varphi}{\partial t}\Big)-\frac{8}{25}l_1^2\left(A_{22}\frac{\partial^5 u}{\partial t\partial x^4}+\frac{A_{22}}{R}\frac{\partial^4 w}{\partial t\partial x^3}+\frac{1}{2}\frac{A_{22}}{R}\frac{\partial^3\varphi}{\partial t\partial x^2}\right.\\+B_{22}\frac{\partial^5\varphi}{\partial t\partial x^4}\Big)-\frac{8}{15}\frac{l_1^2}{R}\left(2A_{22}\frac{\partial^3\varphi}{\partial t\partial x^2}+A_{22}\frac{\partial^4 w}{\partial t\partial x^3}-\frac{A_{22}}{R}\frac{\partial^3 u}{\partial t\partial x^2}\right.\\-\frac{B_{22}}{R}\frac{\partial^3\varphi}{\partial t\partial x^2}\Big)-\frac{12}{25}l_1^2\left(A_{22}\frac{\partial^5 u}{\partial t\partial x^4}+\frac{A_{22}}{R}\frac{\partial^4 w}{\partial t\partial x^3}+B_{22}\frac{\partial^5\varphi}{\partial t\partial x^4}\right)\\-\frac{6}{25}\frac{l_1^2A_{22}}{R}\frac{\partial^3\varphi}{\partial t\partial x^2}-2l_0^2\left(A_{22}\frac{\partial^5 u}{\partial t\partial x^4}+\frac{A_{22}}{R}\frac{\partial^4 w}{\partial t\partial x^3}+B_{22}\frac{\partial^5\varphi}{\partial t\partial x^4}\right)\\+\frac{1}{4}\frac{l_2^2}{R}\left(A_{22}\frac{\partial^3\varphi}{\partial t\partial x^2}-A_{22}\frac{\partial^4 w}{\partial t\partial x^3}+\frac{A_{22}}{R}\frac{\partial^3 u}{\partial t\partial x^2}+\frac{B_{22}}{R}\frac{\partial^3\varphi}{\partial t\partial x^2}\right)\end{pmatrix} \tag{40a}$$
$$=I_1\frac{\partial^2 u}{\partial t^2}-I_2\frac{\partial^2\varphi}{\partial t^2},$$

$$-\frac{1}{R}\left(A_{11}\frac{\partial u}{\partial x}+\frac{A_{11}}{R}w+B_{11}\frac{\partial\varphi}{\partial x}\right)+K_s\left(\frac{A_{22}}{R}\frac{\partial^2 w}{\partial x^2}-\frac{A_{22}}{R}\frac{\partial u}{\partial x}+A_{22}\frac{\partial\varphi}{\partial x}-\frac{B_{22}}{R}\frac{\partial\varphi}{\partial x}\right)$$
$$+\frac{8}{25}\frac{l_1^2}{R}\left(A_{22}\frac{\partial^3 u}{\partial x^3}+\frac{A_{22}}{R}\frac{\partial^2 w}{\partial x^2}+\frac{1}{2}\frac{A_{22}}{R}\frac{\partial\varphi}{\partial x}+B_{22}\frac{\partial^3\varphi}{\partial x^3}\right)-\frac{8}{15}l_1^2\left(2A_{22}\frac{\partial^3\varphi}{\partial x^3}+A_{22}\frac{\partial^4 w}{\partial x^4}\right.$$
$$-\frac{A_{22}}{R}\frac{\partial^3 u}{\partial x^3}-\frac{B_{22}}{R}\frac{\partial^3\varphi}{\partial x^3}\Big)-\frac{3}{5R}\left(-\frac{2}{5}l_1^2\left(A_{22}\frac{\partial^3 u}{\partial x^3}+\frac{A_{22}}{R}\frac{\partial^2 w}{\partial x^2}+B_{22}\frac{\partial^3\varphi}{\partial x^3}\right)+\frac{2}{15}\frac{l_1^2A_{22}}{R}\frac{\partial\varphi}{\partial x}\right)$$
$$-\frac{3}{5R}\left(-\frac{2}{5}l_1^2\left(A_{22}\frac{\partial^3 u}{\partial x^3}+\frac{A_{22}}{R}\frac{\partial^2 w}{\partial x^2}+B_{22}\frac{\partial^3\varphi}{\partial x^3}\right)-\frac{8}{15}\frac{l_1^2A_{22}}{R}\frac{\partial\varphi}{\partial x}\right)$$
$$+\frac{2l_0^2}{R}\left(A_{22}\frac{\partial^3 u}{\partial x^3}+\frac{A_{22}}{R}\frac{\partial^2 w}{\partial x^2}+B_{22}\frac{\partial^3\varphi}{\partial x^3}\right)+\frac{1}{4}l_2^2\left(A_{22}\frac{\partial^3\varphi}{\partial x^3}-A_{22}\frac{\partial^4 w}{\partial x^4}+\frac{A_{22}}{R}\frac{\partial^3 u}{\partial x^3}+\frac{B_{22}}{R}\frac{\partial^3\varphi}{\partial x^3}\right)$$
$$+g\begin{pmatrix}-\frac{1}{R}\left(A_{11}\frac{\partial^2 u}{\partial t\partial x}+\frac{A_{11}}{R}\frac{\partial w}{\partial t}+B_{11}\frac{\partial^2\varphi}{\partial t\partial x}\right)+K_s\left(\frac{A_{22}}{R}\frac{\partial^3 w}{\partial t\partial x^2}-\frac{A_{22}}{R}\frac{\partial^2 u}{\partial t\partial x}\right.\\+A_{22}\frac{\partial^2\varphi}{\partial t\partial x}-\frac{B_{22}}{R}\frac{\partial^2\varphi}{\partial t\partial x}\Big)+\frac{8}{25}\frac{l_1^2}{R}\left(A_{22}\frac{\partial^4 u}{\partial t\partial x^3}+\frac{A_{22}}{R}\frac{\partial^3 w}{\partial t\partial x^2}+\frac{1}{2}\frac{A_{22}}{R}\frac{\partial^2\varphi}{\partial t\partial x}\right.\\+B_{22}\frac{\partial^4\varphi}{\partial t\partial x^3}\Big)-\frac{8}{15}l_1^2\left(2A_{22}\frac{\partial^4\varphi}{\partial t\partial x^3}+A_{22}\frac{\partial^5 w}{\partial t\partial x^4}-\frac{A_{22}}{R}\frac{\partial^4 u}{\partial t\partial x^3}-\frac{B_{22}}{R}\frac{\partial^4\varphi}{\partial t\partial x^3}\right)\\-\frac{3}{5R}\left(-\frac{2}{5}l_1^2\left(A_{22}\frac{\partial^4 u}{\partial t\partial x^3}+\frac{A_{22}}{R}\frac{\partial^3 w}{\partial t\partial x^2}+B_{22}\frac{\partial^4\varphi}{\partial t\partial x^3}\right)+\frac{2}{15}\frac{l_1^2A_{22}}{R}\frac{\partial^2\varphi}{\partial t\partial x}\right)\\-\frac{3}{5R}\left(-\frac{2}{5}l_1^2\left(A_{22}\frac{\partial^4 u}{\partial t\partial x^3}+\frac{A_{22}}{R}\frac{\partial^3 w}{\partial t\partial x^2}+B_{22}\frac{\partial^4\varphi}{\partial t\partial x^3}\right)-\frac{8}{15}\frac{l_1^2A_{22}}{R}\frac{\partial^2\varphi}{\partial t\partial x}\right)\\+\frac{2l_0^2}{R}\left(A_{22}\frac{\partial^4 u}{\partial t\partial x^3}+\frac{A_{22}}{R}\frac{\partial^3 w}{\partial t\partial x^2}+B_{22}\frac{\partial^4\varphi}{\partial t\partial x^3}\right)+\frac{1}{4}l_2^2\left(A_{22}\frac{\partial^4\varphi}{\partial t\partial x^3}-A_{22}\frac{\partial^5 w}{\partial t\partial x^4}\right.\\+\frac{A_{22}}{R}\frac{\partial^4 u}{\partial t\partial x^3}+\frac{B_{22}}{R}\frac{\partial^4\varphi}{\partial t\partial x^3}\Big)\end{pmatrix} \tag{40b}$$
$$+P\frac{\partial^2 w}{\partial x^2}-k_w w+k_g\frac{\partial^2 w}{\partial x^2}+\eta A H_x^2\frac{\partial^2 w}{\partial x^2}-\left(\int_{-h/2}^{h/2}\alpha_{xx}Q_{11}\Delta T\right)\frac{\partial^2 w}{\partial x^2}=I_1\frac{\partial^2 w}{\partial t^2},$$

$$-K_s\left(\frac{A_{22}}{R}\frac{\partial w}{\partial x}-\frac{A_{22}}{R}u+A_{22}\varphi-\frac{B_{22}}{R}\varphi\right)+\frac{16}{15}l_1^2\left(2A_{22}\frac{\partial^2\varphi}{\partial x^2}+A_{22}\frac{\partial^3 w}{\partial x^3}\right.$$
$$-\frac{A_{22}}{R}\frac{\partial^2 u}{\partial x^2}-\frac{B_{22}}{R}\frac{\partial^2\varphi}{\partial x^2}\Big)+\frac{1}{4}l_2^2\left(A_{22}\frac{\partial^2\varphi}{\partial x^2}-A_{22}\frac{\partial^3 w}{\partial x^3}+\frac{A_{22}}{R}\frac{\partial^2 u}{\partial x^2}+\frac{B_{22}}{R}\frac{\partial^2\varphi}{\partial x^2}\right)$$
$$+B_{11}\frac{\partial^2 u}{\partial x^2}+D_{11}\frac{\partial^2\varphi}{\partial x^2}+\frac{1}{R}\left(B_{22}\frac{\partial w}{\partial x}-\frac{B_{22}}{R}u+B_{22}\varphi-\frac{D_{22}}{R}\varphi\right)-\frac{8}{25}l_1^2\left(B_{22}\frac{\partial^4 u}{\partial x^4}\right.$$
$$+\frac{B_{22}}{R}\frac{\partial^3 w}{\partial x^3}+\frac{1}{2}\frac{B_{22}}{R}\frac{\partial^2\varphi}{\partial x^2}+D_{22}\frac{\partial^4\varphi}{\partial x^4}\Big)-\frac{12}{25}l_1^2\left(B_{22}\frac{\partial^4 u}{\partial x^4}+\frac{B_{22}}{R}\frac{\partial^3 w}{\partial x^3}+D_{22}\frac{\partial^4\varphi}{\partial x^4}\right)$$
$$-\frac{1}{5}\left(-\frac{2}{5}l_1^2\left(A_{22}\frac{\partial^2 u}{\partial x^2}+\frac{A_{22}}{R}\frac{\partial w}{\partial x}+B_{22}\frac{\partial^2\varphi}{\partial x^2}\right)+\frac{2}{15}\frac{l_1^2A_{22}}{R}\varphi\right)$$
$$+\frac{4}{5}\left(-\frac{2}{5}l_1^2\left(A_{22}\frac{\partial^2 u}{\partial x^2}+\frac{A_{22}}{R}\frac{\partial w}{\partial x}+B_{22}\frac{\partial^2\varphi}{\partial x^2}\right)-\frac{8}{15}\frac{l_1^2A_{22}}{R}\varphi\right)-2l_0^2\left(B_{22}\frac{\partial^4 u}{\partial x^4}\right.$$
$$+\frac{B_{22}}{R}\frac{\partial^3 w}{\partial x^3}+D_{22}\frac{\partial^4\varphi}{\partial x^4}\Big)-\frac{6}{25}\frac{l_1^2B_{22}}{R}\frac{\partial^2\varphi}{\partial x^2}-\frac{1}{4}\frac{l_2^2A_{22}}{R^2}\varphi-\frac{4}{25}\frac{l_1^2}{R}\left(A_{22}\frac{\partial^2 u}{\partial x^2}\right.$$
$$+\frac{A_{22}}{R}\frac{\partial^3 w}{\partial x^3}+\frac{1}{2}\frac{A_{22}}{R}\frac{\partial^2\varphi}{\partial x^2}+B_{22}\frac{\partial^4\varphi}{\partial x^4}\Big)+2l_0^2A_{22}\frac{\partial^2\varphi}{\partial x^2}+\frac{B_{11}}{R}\frac{\partial w}{\partial x}-\frac{8}{15}\frac{l_1^2}{R}\left(2B_{22}\frac{\partial^2\varphi}{\partial x^2}\right.$$
$$+B_{22}\frac{\partial^3 w}{\partial x^3}-\frac{B_{22}}{R}\frac{\partial^2 u}{\partial x^2}-\frac{D_{22}}{R}\frac{\partial^2\varphi}{\partial x^2}\Big)+\frac{1}{4}\frac{l_2^2}{R}\left(B_{22}\frac{\partial^2\varphi}{\partial x^2}-B_{22}\frac{\partial^3 w}{\partial x^3}+\frac{B_{22}}{R}\frac{\partial^2 u}{\partial x^2}+\frac{D_{22}}{R}\frac{\partial^2\varphi}{\partial x^2}\right)$$
$$+g\begin{pmatrix}-K_s\left(\frac{A_{22}}{R}\frac{\partial^2 w}{\partial t\partial x}-\frac{A_{22}}{R}\frac{\partial u}{\partial t}+A_{22}\varphi-\frac{B_{22}}{R}\frac{\partial\varphi}{\partial t}\right)+\frac{16}{15}l_1^2\left(2A_{22}\frac{\partial^3\varphi}{\partial t\partial x^2}+A_{22}\frac{\partial^4 w}{\partial t\partial x^3}\right.\\-\frac{A_{22}}{R}\frac{\partial^3 u}{\partial t\partial x^2}-\frac{B_{22}}{R}\frac{\partial^3\varphi}{\partial t\partial x^2}\Big)+\frac{1}{4}l_2^2\left(A_{22}\frac{\partial^3\varphi}{\partial t\partial x^2}-A_{22}\frac{\partial^4 w}{\partial t\partial x^3}+\frac{A_{22}}{R}\frac{\partial^3 u}{\partial t\partial x^2}\right.\\+\frac{B_{22}}{R}\frac{\partial^3\varphi}{\partial t\partial x^2}\Big)+B_{11}\frac{\partial^3 u}{\partial t\partial x^2}+D_{11}\frac{\partial^3\varphi}{\partial t\partial x^2}+\frac{1}{R}\left(B_{22}\frac{\partial^2 w}{\partial t\partial x}-\frac{B_{22}}{R}\frac{\partial u}{\partial t}+B_{22}\frac{\partial\varphi}{\partial t}\right.\\-\frac{D_{22}}{R}\frac{\partial\varphi}{\partial t}\Big)-\frac{8}{25}l_1^2\left(B_{22}\frac{\partial^5 u}{\partial t\partial x^4}+\frac{B_{22}}{R}\frac{\partial^4 w}{\partial t\partial x^3}+\frac{1}{2}\frac{B_{22}}{R}\frac{\partial^3\varphi}{\partial t\partial x^2}+D_{22}\frac{\partial^5\varphi}{\partial t\partial x^4}\right)\\-\frac{12}{25}l_1^2\left(B_{22}\frac{\partial^5 u}{\partial t\partial x^4}+\frac{B_{22}}{R}\frac{\partial^4 w}{\partial t\partial x^3}+D_{22}\frac{\partial^5\varphi}{\partial t\partial x^4}\right)\\-\frac{1}{5}\left(-\frac{2}{5}l_1^2\left(A_{22}\frac{\partial^3 u}{\partial t\partial x^2}+\frac{A_{22}}{R}\frac{\partial^2 w}{\partial t\partial x}+B_{22}\frac{\partial^3\varphi}{\partial t\partial x^2}\right)+\frac{2}{15}\frac{l_1^2A_{22}}{R}\frac{\partial\varphi}{\partial t}\right)\\+\frac{4}{5}\left(-\frac{2}{5}l_1^2\left(A_{22}\frac{\partial^3 u}{\partial t\partial x^2}+\frac{A_{22}}{R}\frac{\partial^2 w}{\partial t\partial x}+B_{22}\frac{\partial^3\varphi}{\partial t\partial x^2}\right)-\frac{8}{15}\frac{l_1^2A_{22}}{R}\frac{\partial\varphi}{\partial t}\right)\\-2l_0^2\left(B_{22}\frac{\partial^5 u}{\partial t\partial x^4}+\frac{B_{22}}{R}\frac{\partial^4 w}{\partial t\partial x^3}+D_{22}\frac{\partial^5\varphi}{\partial t\partial x^4}\right)-\frac{6}{25}\frac{l_1^2B_{22}}{R}\frac{\partial^3\varphi}{\partial t\partial x^2}-\frac{1}{4}\frac{l_2^2A_{22}}{R^2}\frac{\partial\varphi}{\partial t}\\-\frac{4}{25}\frac{l_1^2}{R}\left(A_{22}\frac{\partial^3 u}{\partial t\partial x^2}+\frac{A_{22}}{R}\frac{\partial^4 w}{\partial t\partial x^3}+\frac{1}{2}\frac{A_{22}}{R}\frac{\partial^3\varphi}{\partial t\partial x^2}+B_{22}\frac{\partial^5\varphi}{\partial t\partial x^4}\right)\\+2l_0^2A_{22}\frac{\partial^3\varphi}{\partial t\partial x^2}+\frac{B_{11}}{R}\frac{\partial^2 w}{\partial t\partial x}-\frac{8}{15}\frac{l_1^2}{R}\left(2B_{22}\frac{\partial^3\varphi}{\partial t\partial x^2}+B_{22}\frac{\partial^4 w}{\partial t\partial x^3}-\frac{B_{22}}{R}\frac{\partial^3 u}{\partial t\partial x^2}\right.\\-\frac{D_{22}}{R}\frac{\partial^3\varphi}{\partial t\partial x^2}\Big)+\frac{1}{4}\frac{l_2^2}{R}\left(B_{22}\frac{\partial^3\varphi}{\partial t\partial x^2}-B_{22}\frac{\partial^4 w}{\partial t\partial x^3}+\frac{B_{22}}{R}\frac{\partial^3 u}{\partial t\partial x^2}+\frac{D_{22}}{R}\frac{\partial^3\varphi}{\partial t\partial x^2}\right)\end{pmatrix} \tag{40c}$$
$$=I_3\frac{\partial^2\varphi}{\partial t^2}-I_2\frac{\partial^2 u}{\partial t^2}.$$

where

$$\{A_{11},B_{11},D_{11}\}=\int_{-h/2}^{h/2}Q_{11}(z)\{1,z,z^2\}dz, \tag{41}$$

$$\{A_{22},B_{22},D_{22}\}=\int_{-h/2}^{h/2}Q_{12}(z)\{1,z,z^2\}dz, \tag{42}$$

3.6 Boundary conditions

Three different size-dependent boundary conditions at both ends of the nanocomposite curved microbeams, including Simply Supported-Simply Supported (SS), Clamped-Clamped (CC) and Clamped-Simply Supported (CS) are considered which can be expressed as follows

For case (SS)
At $x = 0, L$

$$w=\frac{\partial u}{\partial x}=\frac{\partial\varphi}{\partial x}=0, \tag{43a}$$

$$
\begin{aligned}
&-A_{11}\frac{\partial u}{\partial x}-\frac{A_{11}}{R}w-B_{11}\frac{\partial \varphi}{\partial x}+\frac{8}{25}l_1^2\left(A_{22}\frac{\partial^3 u}{\partial x^3}+\frac{A_{22}}{R}\frac{\partial^2 w}{\partial x^2}+\frac{1}{2}\frac{A_{22}}{R}\frac{\partial \varphi}{\partial x}\right.\\
&\left.+B_{22}\frac{\partial^3 \varphi}{\partial x^3}\right)+\frac{8}{15}\frac{l_1^2}{R}\left(2A_{22}\frac{\partial \varphi}{\partial x}+A_{22}\frac{\partial^2 w}{\partial x^2}-\frac{A_{22}}{R}\frac{\partial u}{\partial x}-\frac{B_{22}}{R}\frac{\partial \varphi}{\partial x}\right)\\
&+\frac{12}{25}l_1^2\left(A_{22}\frac{\partial^3 u}{\partial x^3}+\frac{A_{22}}{R}\frac{\partial^2 w}{\partial x^2}+B_{22}\frac{\partial^3 \varphi}{\partial x^3}\right)+\frac{6}{25}\frac{l_1^2A_{22}}{R}\frac{\partial \varphi}{\partial x}+2l_0^2\left(A_{22}\frac{\partial^3 u}{\partial x^3}\right.\\
&\left.+\frac{A_{22}}{R}\frac{\partial^2 w}{\partial x^2}+B_{22}\frac{\partial^3 \varphi}{\partial x^3}\right)-\frac{1}{4}\frac{l_2^2}{R}\left(A_{22}\frac{\partial \varphi}{\partial x}-A_{22}\frac{\partial^2 w}{\partial x^2}+\frac{A_{22}}{R}\frac{\partial u}{\partial x}+\frac{B_{22}}{R}\frac{\partial \varphi}{\partial x}\right)\\
&+g\begin{pmatrix}
-A_{11}\dfrac{\partial^2 u}{\partial t\partial x}-\dfrac{A_{11}}{R}\dfrac{\partial w}{\partial t}-B_{11}\dfrac{\partial^2 \varphi}{\partial t\partial x}+\dfrac{8}{25}l_1^2\left(A_{22}\dfrac{\partial^4 u}{\partial t\partial x^3}+\dfrac{A_{22}}{R}\dfrac{\partial^3 w}{\partial t\partial x^2}\right.\\
\left.+\dfrac{1}{2}\dfrac{A_{22}}{R}\dfrac{\partial^2 \varphi}{\partial t\partial x}+B_{22}\dfrac{\partial^4 \varphi}{\partial t\partial x^3}\right)+\dfrac{8}{15}\dfrac{l_1^2}{R}\left(2A_{22}\dfrac{\partial^2 \varphi}{\partial t\partial x}+A_{22}\dfrac{\partial^3 w}{\partial t\partial x^2}\right.\\
\left.-\dfrac{A_{22}}{R}\dfrac{\partial^2 u}{\partial t\partial x}-\dfrac{B_{22}}{R}\dfrac{\partial^2 \varphi}{\partial t\partial x}\right)+\dfrac{12}{25}l_1^2\left(A_{22}\dfrac{\partial^4 u}{\partial t\partial x^3}+\dfrac{A_{22}}{R}\dfrac{\partial^3 w}{\partial t\partial x^2}+B_{22}\dfrac{\partial^4 \varphi}{\partial t\partial x^3}\right)\\
+\dfrac{6}{25}\dfrac{l_1^2A_{22}}{R}\dfrac{\partial^2 \varphi}{\partial t\partial x}+2l_0^2\left(A_{22}\dfrac{\partial^4 u}{\partial t\partial x^3}+\dfrac{A_{22}}{R}\dfrac{\partial^3 w}{\partial t\partial x^2}+B_{22}\dfrac{\partial^4 \varphi}{\partial t\partial x^3}\right)\\
-\dfrac{1}{4}\dfrac{l_2^2}{R}\left(A_{22}\dfrac{\partial^2 \varphi}{\partial t\partial x}-A_{22}\dfrac{\partial^3 w}{\partial t\partial x^2}+\dfrac{A_{22}}{R}\dfrac{\partial^2 u}{\partial t\partial x}+\dfrac{B_{22}}{R}\dfrac{\partial^2 \varphi}{\partial t\partial x}\right)
\end{pmatrix}=0,
\end{aligned}
\tag{43b}
$$

$$
\begin{aligned}
&-B_{11}\frac{\partial u}{\partial x}-\frac{B_{11}}{R}w-D_{11}\frac{\partial \varphi}{\partial x}+\frac{8}{25}\frac{l_1^2}{R}\left(B_{22}\frac{\partial^3 u}{\partial x^3}+\frac{B_{22}}{R}\frac{\partial^2 w}{\partial x^2}+\frac{1}{2}\frac{B_{22}}{R}\frac{\partial \varphi}{\partial x}\right.\\
&\left.+D_{22}\frac{\partial^3 \varphi}{\partial x^3}\right)-\frac{16}{15}l_1^2\left(2A_{22}\frac{\partial \varphi}{\partial x}+A_{22}\frac{\partial^2 w}{\partial x^2}-\frac{A_{22}}{R}\frac{\partial u}{\partial x}-\frac{B_{22}}{R}\frac{\partial \varphi}{\partial x}\right)\\
&+\frac{8}{15}\frac{l_1^2}{R}\left(2B_{22}\frac{\partial \varphi}{\partial x}+B_{22}\frac{\partial^2 w}{\partial x^2}-\frac{B_{22}}{R}\frac{\partial u}{\partial x}-\frac{D_{22}}{R}\frac{\partial \varphi}{\partial x}\right)+\frac{6}{25}l_1^2\left(B_{22}\frac{\partial^3 u}{\partial x^3}\right.\\
&\left.+\frac{B_{22}}{R}\frac{\partial^2 w}{\partial x^2}+D_{22}\frac{\partial^3 \varphi}{\partial x^3}\right)+\frac{8}{25}\frac{l_1^2B_{22}}{R}\frac{\partial \varphi}{\partial x}+2l_0^2\left(B_{22}\frac{\partial^3 u}{\partial x^3}+\frac{B_{22}}{R}\frac{\partial^2 w}{\partial x^2}\right.\\
&\left.+D_{22}\frac{\partial^3 \varphi}{\partial x^3}\right)-2l_0^2A_{22}\frac{\partial \varphi}{\partial x}-\frac{1}{4}l_2^2\left(A_{22}\frac{\partial \varphi}{\partial x}-A_{22}\frac{\partial^2 w}{\partial x^2}+\frac{A_{22}}{R}\frac{\partial u}{\partial x}+\frac{B_{22}}{R}\frac{\partial \varphi}{\partial x}\right)\\
&-\frac{1}{4}\frac{l_2^2}{R}\left(B_{22}\frac{\partial \varphi}{\partial x}-B_{22}\frac{\partial^2 w}{\partial x^2}+\frac{B_{22}}{R}\frac{\partial u}{\partial x}+\frac{D_{22}}{R}\frac{\partial \varphi}{\partial x}\right)\\
&+g\begin{pmatrix}
B_{11}\dfrac{\partial^2 u}{\partial t\partial x}-\dfrac{B_{11}}{R}\dfrac{\partial w}{\partial t}-D_{11}\dfrac{\partial^2 \varphi}{\partial t\partial x}+\dfrac{8}{25}\dfrac{l_1^2}{R}\left(B_{22}\dfrac{\partial^4 u}{\partial t\partial x^3}+\dfrac{B_{22}}{R}\dfrac{\partial^3 w}{\partial t\partial x^2}\right.\\
\left.+\dfrac{1}{2}\dfrac{B_{22}}{R}\dfrac{\partial^2 \varphi}{\partial t\partial x}+D_{22}\dfrac{\partial^4 \varphi}{\partial t\partial x^3}\right)-\dfrac{16}{15}l_1^2\left(2A_{22}\dfrac{\partial^2 \varphi}{\partial t\partial x}+A_{22}\dfrac{\partial^3 w}{\partial t\partial x^2}-\dfrac{A_{22}}{R}\dfrac{\partial^2 u}{\partial t\partial x}\right.\\
\left.-\dfrac{B_{22}}{R}\dfrac{\partial^2 \varphi}{\partial t\partial x}\right)+\dfrac{8}{15}\dfrac{l_1^2}{R}\left(2B_{22}\dfrac{\partial^2 \varphi}{\partial t\partial x}+B_{22}\dfrac{\partial^3 w}{\partial t\partial x^2}-\dfrac{B_{22}}{R}\dfrac{\partial^2 u}{\partial t\partial x}-\dfrac{D_{22}}{R}\dfrac{\partial^2 \varphi}{\partial t\partial x}\right)\\
+\dfrac{6}{25}l_1^2\left(B_{22}\dfrac{\partial^4 u}{\partial t\partial x^3}+\dfrac{B_{22}}{R}\dfrac{\partial^3 w}{\partial t\partial x^2}+D_{22}\dfrac{\partial^4 \varphi}{\partial t\partial x^3}\right)+\dfrac{8}{25}\dfrac{l_1^2B_{22}}{R}\dfrac{\partial^2 \varphi}{\partial t\partial x}\\
+2l_0^2\left(B_{22}\dfrac{\partial^4 u}{\partial t\partial x^3}+\dfrac{B_{22}}{R}\dfrac{\partial^3 w}{\partial t\partial x^2}+D_{22}\dfrac{\partial^4 \varphi}{\partial t\partial x^3}\right)-2l_0^2A_{22}\dfrac{\partial^2 \varphi}{\partial t\partial x}\\
-\dfrac{1}{4}l_2^2\left(A_{22}\dfrac{\partial^2 \varphi}{\partial t\partial x}-A_{22}\dfrac{\partial^3 w}{\partial t\partial x^2}+\dfrac{A_{22}}{R}\dfrac{\partial^2 u}{\partial t\partial x}+\dfrac{B_{22}}{R}\dfrac{\partial^2 \varphi}{\partial t\partial x}\right)-\dfrac{1}{4}\dfrac{l_2^2}{R}\left(B_{22}\dfrac{\partial^2 \varphi}{\partial t\partial x}\right.\\
\left.-B_{22}\dfrac{\partial^3 w}{\partial t\partial x^2}+\dfrac{B_{22}}{R}\dfrac{\partial^2 u}{\partial t\partial x}+\dfrac{D_{22}}{R}\dfrac{\partial^2 \varphi}{\partial t\partial x}\right)
\end{pmatrix}=0,
\end{aligned}
\tag{43c}
$$

$$
\begin{aligned}
&-\frac{34}{75}l_1^2\left(2A_{22}\frac{\partial \varphi}{\partial x}+A_{22}\frac{\partial^2 w}{\partial x^2}-\frac{A_{22}}{R}\frac{\partial u}{\partial x}-\frac{B_{22}}{R}\frac{\partial \varphi}{\partial x}\right)\\
&+\frac{1}{4}l_2^2\left(A_{22}\frac{\partial \varphi}{\partial x}-A_{22}\frac{\partial^2 w}{\partial x^2}+\frac{A_{22}}{R}\frac{\partial u}{\partial x}+\frac{B_{22}}{R}\frac{\partial \varphi}{\partial x}\right)\\
&+g\begin{pmatrix}
-\dfrac{34}{75}l_1^2\left(2A_{22}\dfrac{\partial^2 \varphi}{\partial t\partial x}+A_{22}\dfrac{\partial^3 w}{\partial t\partial x^2}-\dfrac{A_{22}}{R}\dfrac{\partial^2 u}{\partial t\partial x}-\dfrac{B_{22}}{R}\dfrac{\partial^2 \varphi}{\partial t\partial x}\right)\\
+\dfrac{1}{4}l_2^2\left(A_{22}\dfrac{\partial^2 \varphi}{\partial t\partial x}-A_{22}\dfrac{\partial^3 w}{\partial t\partial x^2}+\dfrac{A_{22}}{R}\dfrac{\partial^2 u}{\partial t\partial x}+\dfrac{B_{22}}{R}\dfrac{\partial^2 \varphi}{\partial t\partial x}\right)
\end{pmatrix}=0.
\end{aligned}
\tag{43d}
$$

For case (CC)
At $x=0, L$

$$
u=w=\varphi=\frac{\partial u}{\partial x}=\frac{\partial w}{\partial x}=\frac{\partial \varphi}{\partial x}=0. \tag{44}
$$

For case (CS)
At $x=0$

$$
u=w=\varphi=\frac{\partial u}{\partial x}=\frac{\partial w}{\partial x}=\frac{\partial \varphi}{\partial x}=0 \tag{45}
$$

At $x=L$

$$
w=\frac{\partial u}{\partial x}=\frac{\partial \varphi}{\partial x}=0, \tag{46a}
$$

$$
\begin{aligned}
&-A_{11}\frac{\partial u}{\partial x}-\frac{A_{11}}{R}w-B_{11}\frac{\partial \varphi}{\partial x}+\frac{8}{25}l_1^2\left(A_{22}\frac{\partial^3 u}{\partial x^3}+\frac{A_{22}}{R}\frac{\partial^2 w}{\partial x^2}+\frac{1}{2}\frac{A_{22}}{R}\frac{\partial \varphi}{\partial x}\right.\\
&\left.+B_{22}\frac{\partial^3 \varphi}{\partial x^3}\right)+\frac{8}{15}\frac{l_1^2}{R}\left(2A_{22}\frac{\partial \varphi}{\partial x}+A_{22}\frac{\partial^2 w}{\partial x^2}-\frac{A_{22}}{R}\frac{\partial u}{\partial x}-\frac{B_{22}}{R}\frac{\partial \varphi}{\partial x}\right)\\
&+\frac{12}{25}l_1^2\left(A_{22}\frac{\partial^3 u}{\partial x^3}+\frac{A_{22}}{R}\frac{\partial^2 w}{\partial x^2}+B_{22}\frac{\partial^3 \varphi}{\partial x^3}\right)+\frac{6}{25}\frac{l_1^2A_{22}}{R}\frac{\partial \varphi}{\partial x}+2l_0^2\left(A_{22}\frac{\partial^3 u}{\partial x^3}\right.\\
&\left.+\frac{A_{22}}{R}\frac{\partial^2 w}{\partial x^2}+B_{22}\frac{\partial^3 \varphi}{\partial x^3}\right)-\frac{1}{4}\frac{l_2^2}{R}\left(A_{22}\frac{\partial \varphi}{\partial x}-A_{22}\frac{\partial^2 w}{\partial x^2}+\frac{A_{22}}{R}\frac{\partial u}{\partial x}+\frac{B_{22}}{R}\frac{\partial \varphi}{\partial x}\right)\\
&+g\begin{pmatrix}
-A_{11}\dfrac{\partial^2 u}{\partial t\partial x}-\dfrac{A_{11}}{R}\dfrac{\partial w}{\partial t}-B_{11}\dfrac{\partial^2 \varphi}{\partial t\partial x}+\dfrac{8}{25}l_1^2\left(A_{22}\dfrac{\partial^4 u}{\partial t\partial x^3}+\dfrac{A_{22}}{R}\dfrac{\partial^3 w}{\partial t\partial x^2}\right.\\
\left.+\dfrac{1}{2}\dfrac{A_{22}}{R}\dfrac{\partial^2 \varphi}{\partial t\partial x}+B_{22}\dfrac{\partial^4 \varphi}{\partial t\partial x^3}\right)+\dfrac{8}{15}\dfrac{l_1^2}{R}\left(2A_{22}\dfrac{\partial^2 \varphi}{\partial t\partial x}+A_{22}\dfrac{\partial^3 w}{\partial t\partial x^2}\right.\\
\left.-\dfrac{A_{22}}{R}\dfrac{\partial^2 u}{\partial t\partial x}-\dfrac{B_{22}}{R}\dfrac{\partial^2 \varphi}{\partial t\partial x}\right)+\dfrac{12}{25}l_1^2\left(A_{22}\dfrac{\partial^4 u}{\partial t\partial x^3}+\dfrac{A_{22}}{R}\dfrac{\partial^3 w}{\partial t\partial x^2}+B_{22}\dfrac{\partial^4 \varphi}{\partial t\partial x^3}\right)\\
+\dfrac{6}{25}\dfrac{l_1^2A_{22}}{R}\dfrac{\partial^2 \varphi}{\partial t\partial x}+2l_0^2\left(A_{22}\dfrac{\partial^4 u}{\partial t\partial x^3}+\dfrac{A_{22}}{R}\dfrac{\partial^3 w}{\partial t\partial x^2}+B_{22}\dfrac{\partial^4 \varphi}{\partial t\partial x^3}\right)\\
-\dfrac{1}{4}\dfrac{l_2^2}{R}\left(A_{22}\dfrac{\partial^2 \varphi}{\partial t\partial x}-A_{22}\dfrac{\partial^3 w}{\partial t\partial x^2}+\dfrac{A_{22}}{R}\dfrac{\partial^2 u}{\partial t\partial x}+\dfrac{B_{22}}{R}\dfrac{\partial^2 \varphi}{\partial t\partial x}\right)
\end{pmatrix}=0,
\end{aligned}
\tag{46b}
$$

$$
\begin{aligned}
&-B_{11}\frac{\partial u}{\partial x}-\frac{B_{11}}{R}w-D_{11}\frac{\partial \varphi}{\partial x}+\frac{8}{25}\frac{l_1^2}{R}\left(B_{22}\frac{\partial^3 u}{\partial x^3}+\frac{B_{22}}{R}\frac{\partial^2 w}{\partial x^2}+\frac{1}{2}\frac{B_{22}}{R}\frac{\partial \varphi}{\partial x}\right.\\
&\left.+D_{22}\frac{\partial^3 \varphi}{\partial x^3}\right)-\frac{16}{15}l_1^2\left(2A_{22}\frac{\partial \varphi}{\partial x}+A_{22}\frac{\partial^2 w}{\partial x^2}-\frac{A_{22}}{R}\frac{\partial u}{\partial x}-\frac{B_{22}}{R}\frac{\partial \varphi}{\partial x}\right)\\
&+\frac{8}{15}\frac{l_1^2}{R}\left(2B_{22}\frac{\partial \varphi}{\partial x}+B_{22}\frac{\partial^2 w}{\partial x^2}-\frac{B_{22}}{R}\frac{\partial u}{\partial x}-\frac{D_{22}}{R}\frac{\partial \varphi}{\partial x}\right)+\frac{6}{25}l_1^2\left(B_{22}\frac{\partial^3 u}{\partial x^3}\right.\\
&\left.+\frac{B_{22}}{R}\frac{\partial^2 w}{\partial x^2}+D_{22}\frac{\partial^3 \varphi}{\partial x^3}\right)+\frac{8}{25}\frac{l_1^2B_{22}}{R}\frac{\partial \varphi}{\partial x}+2l_0^2\left(B_{22}\frac{\partial^3 u}{\partial x^3}+\frac{B_{22}}{R}\frac{\partial^2 w}{\partial x^2}\right.\\
&\left.+D_{22}\frac{\partial^3 \varphi}{\partial x^3}\right)-2l_0^2A_{22}\frac{\partial \varphi}{\partial x}-\frac{1}{4}l_2^2\left(A_{22}\frac{\partial \varphi}{\partial x}-A_{22}\frac{\partial^2 w}{\partial x^2}+\frac{A_{22}}{R}\frac{\partial u}{\partial x}+\frac{B_{22}}{R}\frac{\partial \varphi}{\partial x}\right)\\
&-\frac{1}{4}\frac{l_2^2}{R}\left(B_{22}\frac{\partial \varphi}{\partial x}-B_{22}\frac{\partial^2 w}{\partial x^2}+\frac{B_{22}}{R}\frac{\partial u}{\partial x}+\frac{D_{22}}{R}\frac{\partial \varphi}{\partial x}\right)\\
&+g\begin{pmatrix}
B_{11}\dfrac{\partial^2 u}{\partial t\partial x}-\dfrac{B_{11}}{R}\dfrac{\partial w}{\partial t}-D_{11}\dfrac{\partial^2 \varphi}{\partial t\partial x}+\dfrac{8}{25}\dfrac{l_1^2}{R}\left(B_{22}\dfrac{\partial^4 u}{\partial t\partial x^3}+\dfrac{B_{22}}{R}\dfrac{\partial^3 w}{\partial t\partial x^2}\right.\\
\left.+\dfrac{1}{2}\dfrac{B_{22}}{R}\dfrac{\partial^2 \varphi}{\partial t\partial x}+D_{22}\dfrac{\partial^4 \varphi}{\partial t\partial x^3}\right)-\dfrac{16}{15}l_1^2\left(2A_{22}\dfrac{\partial^2 \varphi}{\partial t\partial x}+A_{22}\dfrac{\partial^3 w}{\partial t\partial x^2}-\dfrac{A_{22}}{R}\dfrac{\partial^2 u}{\partial t\partial x}\right.\\
\left.-\dfrac{B_{22}}{R}\dfrac{\partial^2 \varphi}{\partial t\partial x}\right)+\dfrac{8}{15}\dfrac{l_1^2}{R}\left(2B_{22}\dfrac{\partial^2 \varphi}{\partial t\partial x}+B_{22}\dfrac{\partial^3 w}{\partial t\partial x^2}-\dfrac{B_{22}}{R}\dfrac{\partial^2 u}{\partial t\partial x}-\dfrac{D_{22}}{R}\dfrac{\partial^2 \varphi}{\partial t\partial x}\right)\\
+\dfrac{6}{25}l_1^2\left(B_{22}\dfrac{\partial^4 u}{\partial t\partial x^3}+\dfrac{B_{22}}{R}\dfrac{\partial^3 w}{\partial t\partial x^2}+D_{22}\dfrac{\partial^4 \varphi}{\partial t\partial x^3}\right)+\dfrac{8}{25}\dfrac{l_1^2B_{22}}{R}\dfrac{\partial^2 \varphi}{\partial t\partial x}\\
+2l_0^2\left(B_{22}\dfrac{\partial^4 u}{\partial t\partial x^3}+\dfrac{B_{22}}{R}\dfrac{\partial^3 w}{\partial t\partial x^2}+D_{22}\dfrac{\partial^4 \varphi}{\partial t\partial x^3}\right)-2l_0^2A_{22}\dfrac{\partial^2 \varphi}{\partial t\partial x}\\
-\dfrac{1}{4}l_2^2\left(A_{22}\dfrac{\partial^2 \varphi}{\partial t\partial x}-A_{22}\dfrac{\partial^3 w}{\partial t\partial x^2}+\dfrac{A_{22}}{R}\dfrac{\partial^2 u}{\partial t\partial x}+\dfrac{B_{22}}{R}\dfrac{\partial^2 \varphi}{\partial t\partial x}\right)-\dfrac{1}{4}\dfrac{l_2^2}{R}\left(B_{22}\dfrac{\partial^2 \varphi}{\partial t\partial x}\right.\\
\left.-B_{22}\dfrac{\partial^3 w}{\partial t\partial x^2}+\dfrac{B_{22}}{R}\dfrac{\partial^2 u}{\partial t\partial x}+\dfrac{D_{22}}{R}\dfrac{\partial^2 \varphi}{\partial t\partial x}\right)
\end{pmatrix}=0,
\end{aligned}
\tag{46c}
$$

$$
\begin{aligned}
&-\frac{34}{75}l_1^2\left(2A_{22}\frac{\partial \varphi}{\partial x}+A_{22}\frac{\partial^2 w}{\partial x^2}-\frac{A_{22}}{R}\frac{\partial u}{\partial x}-\frac{B_{22}}{R}\frac{\partial \varphi}{\partial x}\right)\\
&+\frac{1}{4}l_2^2\left(A_{22}\frac{\partial \varphi}{\partial x}-A_{22}\frac{\partial^2 w}{\partial x^2}+\frac{A_{22}}{R}\frac{\partial u}{\partial x}+\frac{B_{22}}{R}\frac{\partial \varphi}{\partial x}\right)\\
&+g\begin{pmatrix}
-\dfrac{34}{75}l_1^2\left(2A_{22}\dfrac{\partial^2 \varphi}{\partial t\partial x}+A_{22}\dfrac{\partial^3 w}{\partial t\partial x^2}-\dfrac{A_{22}}{R}\dfrac{\partial^2 u}{\partial t\partial x}-\dfrac{B_{22}}{R}\dfrac{\partial^2 \varphi}{\partial t\partial x}\right)\\
+\dfrac{1}{4}l_2^2\left(A_{22}\dfrac{\partial^2 \varphi}{\partial t\partial x}-A_{22}\dfrac{\partial^3 w}{\partial t\partial x^2}+\dfrac{A_{22}}{R}\dfrac{\partial^2 u}{\partial t\partial x}+\dfrac{B_{22}}{R}\dfrac{\partial^2 \varphi}{\partial t\partial x}\right)
\end{pmatrix}=0.
\end{aligned}
\tag{46d}
$$

4. Solution procedure

This paper employs the DQM to solve the governing equations of the microbeam. According to the DQM, the derivative of a function with respect to a space variable at a given discrete point is approximated using a weighted linear sum of the function values at all discrete points in the domain. Therefore, the governing differential equations can be turned into a set of first order algebraic equations. The one-dimensional derivative of the function can be considered as follows (Kolahchi and Moniribidgoli 2016, Kolahchi *et al*. 2016a-b, 2017)

$$\frac{d^n f(x_i)}{dx^n} = \sum_{j=1}^{N} C_{ij}^{(n)} f(x_j) \qquad n = 1,...,N-1. \tag{47}$$

in which $f(x)$ denotes the mentioned function, x_i indicates a sample point of the function domain, N represent number of grid points, f_i is the value of the function at ith sample point and C_{ij} denote the weighting coefficients. So, choosing the grid points and weighting coefficients plays an important role in the accuracy of the results. The grid points are defined based on Chebyshev polynomials which can be considered as below

$$X_i = \frac{L}{2}\left[1-\cos\left(\frac{i-1}{N_x-1}\right)\pi\right], i = 1,...,N_x \tag{48}$$

According to Eq. (48), the grid points are considered so that are closer together near the borders and are far away from each other in distant parts of the borders.

The weighting coefficients can be determined through the following simple algebraic relations

$$A_{ij}^{(1)} = \begin{cases} \dfrac{M(x_i)}{M(x_j)(x_i - x_j)} & for \quad i \neq j, \quad i,j = 1,2,...,N_x, \\ -\sum\limits_{\substack{j=1 \\ i \neq j}}^{N_x} A_{ij}^{(1)} & for \quad i = j, \quad i,j = 1,2,...,N_x \end{cases} \tag{49}$$

in which

$$M(x_i) = \prod_{\substack{j=1 \\ j \neq i}}^{N_x} (x_i - x_j) \tag{50}$$

In addition, the higher-order derivatives are defined as

$$A_{ij}^{(n)} = n\left(A_{ii}^{(n-1)} A_{ij}^{(1)} - \pi ctg\left(\frac{x_i - x_j}{2}\right)\pi\right) \tag{51}$$

Considering the grid points in the domain based on Eq. (48) and substituting Eqs. (47) into the governing Eqs. (40a)-(40c), the eigenvalue problem can be obtained as the following form

$$\left([K]\begin{Bmatrix}\{d_b\}\\ \{d_d\}\end{Bmatrix} + [C]\begin{Bmatrix}\{\dot{d}_b\}\\ \{\dot{d}_d\}\end{Bmatrix} + [M]\begin{Bmatrix}\{\ddot{d}_b\}\\ \{\ddot{d}_d\}\end{Bmatrix}\right) = \begin{Bmatrix}\{0\}\\ \{0\}\end{Bmatrix}, \tag{52}$$

where $[K]$, $[C]$ and $[M]$ are stiffness matrix, damp coefficient matrix and the mass matrix, respectively. Also, $\{d_b\}$ and $\{d_d\}$ are the vectors contained boundary and domain points, respectively. To simplify the solution procedure, Eq. (52) can be reduced to the standard form of eigenvalue problem. For this purpose, Eq. (52) takes the following first order variable as

$$\{\dot{Z}\} = [A]\{Z\}, \tag{53}$$

in which Z and $[A]$ represent the state vector and state matrix, respectively which are defined as

$$Z = \begin{Bmatrix} d_d \\ \dot{d}_d \end{Bmatrix} \quad \text{and} \quad [A] = \begin{bmatrix} [0] & [I] \\ -[M^{-1}K] & -[M^{-1}C] \end{bmatrix}, \tag{54}$$

in which [0] and [I] indicate the zero and unitary matrices, respectively. It should be noted that the existence of the damping because of the structural damping, leads to yield the complex frequencies from the solution of Eq. (53). Therefore, the results consist of two real and imaginary parts. The real part is related to the system damping, and the imaginary part indicates the system frequencies.

5. Numerical results

To study the effects of various parameters on the vibration behavior of the structure, a nanocomposite curved microbeam with central angle of $\theta = \pi/4$, length to thickness ratio of L/h = 20 and thickness to material length scale parameter of h/l = 2 is considered. It should be noted that Lam *et al*. (2003) obtained the material length scale parameter for the homogeneous epoxy beam experimentally as l = 17.6 μm. However, since no experimental data are available for the nanocomposite curved microbeam at present, in order to quantitatively analyze of the structure, the corresponding length scale parameter is considered as $l = l_0 = l_1 = l_2$ = 15 μm in this work. The nanocomposite curved microbeam is made from Poly methyl methacrylate (PMMA) as the matrix material with Poisson's ratios of ν_m = 0.34, temperature-dependent thermal coefficient of $\alpha_m = (1 + 0.0005\Delta T) \times 10^{-6}/K$, and temperature-dependent Young moduli of $E_m = (3.52 - 0.0034T)$ GPa so that $T = T_0 + \Delta T$ and T_0 = 300 K (room temperature). (10, 10) SWCNTs is employed as the reinforcement with the material properties listed in Table 1. Also, the elastic medium is made of Poly

Table 1 Temperature-dependent material properties of (10, 10) SWCNT (L = 9.26 nm, R = 0.68 nm, h = 0.067 nm, υ_{12}^{CNT} = 0.175)

V_{CNT}	MD (Zhang *et al*. 2015)		Rule of mixture			η_2
	E_{11} (GPa)	E_{22} (GPa)	E_{11} (GPa)	η_1	E_{22} (GPa)	
0.11	94.8	2.2	94.57	0.149	2.2	0.934
0.14	120.2	2.3	120.09	0.150	2.3	0.942
0.17	145.6	3.5	145.08	0.149	3.5	1.381

Table 2 Convergence and accuracy of DQM for eigenvalues of nanocomposite micro curved beam for different boundary conditions and damper constant of viscoelastic medium

N		SS		SC		CC	
		$C_D=0$	$C_D=10$	$C_D=0$	$C_D=10$	$C_D=0$	$C_D=10$
7	Im (Ω)	2.1143	0.5512	3.7718	2.2081	3.0012	2.1124
	Re (Ω)	-1.5181	-5.1231	-2.2012	-3.8812	-1.5418	-3.6617
		-1.5181	-5.1231	-2.2012	-3.8812	-1.5418	-3.6617
11	Im (Ω)	1.5981	0	2.8901	1.7123	2.5871	1.6112
	Re (Ω)	-1.0888	-4.8901	-1.8001	-3.3126	-1.0908	-3.1222
		-1.0888	-1.7112	-1.8001	-3.3126	-1.0908	-3.1222
15	Im (Ω)	1.5374	0	2.2244	1.0185	2.5253	1.5625
	Re (Ω)	-1.0216	-4.3424	-1.0283	-2.9784	-1.0315	-2.9915
		-1.0216	-1.6925	-1.0283	-2.9784	-1.0315	-2.9915
17	Im (Ω)	1.5372	0	2.2241	1.0181	2.5251	1.5621
	Re (Ω)	-1.0212	-4.3421	-1.0281	-2.9781	-1.031	-2.9912
		-1.0212	-1.6923	-1.0281	-2.9781	-1.031	-2.9912
	ξ	0.5533	1.0810	0.4195	0.3782	0.9721	0.9144

dimethylsiloxane (PDMS) with Poisson's ratios of v_s = 0.48and Young moduli of E_s = (3.22 – 0.0034T) GPa (Zhang *et al*. 2015).

5.1 Convergence of DQM

In this section, convergence and accuracy analysis are carried out to determine the minimum number of grid points required to achieve the stable and accurate results. In Table 2 the dimensionless ($\Omega = \omega L\sqrt{I_1 / A_{11}}$) eigenvalues of the nanocomposite curved microbeam are listed for different boundary conditions and damper constant of viscoelastic medium. As can be observed, the sufficient number of grid points which yields the accurate results for the present work is seventeen (N = 17) for different boundary conditions.

5.2 Validation

To ensure the accuracy and validation of the present study, the frequencies of the SS nanocomposite curved microbeam calculated by the DQM are compared with the results obtained from exact solution. A close agreement between the results of these two methods can be observed from Fig. 2 which demonstrates validation of the present work.

5.3 The effect of different parameters

In this part, the effects of parameters such as volume percent and distribution type of CNTs, temperature change, magnetic field, boundary conditions, material length scale parameter, central angle, viscoelastic medium and structural damping on the frequency of the structure are examined. Fig. 3 shows the effect of various boundary conditions on the non-dimensional eigenfrequency parameter and damping ratio versus different values of non-dimensional damper constant ($C_D = c_d L / h^2\sqrt{\rho_m E_m}$). It can be seen that with increasing the damper constant, the imaginary part of the eigenfrequency decreases for all boundary conditions types. It is also observed that with increasing the damper constant, the imaginary part of eigenfrequency becomes zero for SS and CS boundary conditions which mean that the system is critically damped while for CC boundary condition this situation will be occurred at higher values of damper constant (see Fig. 3(a)). Furthermore, the effect of the damper constant on the real part of eigenfrequency is depicted in Fig. 3(b). It is apparent that the structure with SS or CS boundary condition is critically damped at the lower values of damper constant with respect to the structure with CC boundary condition. This indicates that CC boundary condition restricts the displacements of the structure and thus increases the stiffness of the system more than two other boundary conditions. From Fig. 3c, three regions, including under-damped ($0 < \xi < 1$), critically damped ($\xi = 1$) and over-damped ($\xi > 1$) can be observed.

The effect of CNTs distribution types on the eigenfrequency and the damping ratio of the structure is plotted in Fig. 4. As can be seen, the highest frequency belongs to the structure with FGX distribution type of CNTs while the lowest one can be predicted for FGO distribution type. Therefore, the structure with FGX distribution type has higher stiffness and after that UD, FGA and FGO ones, respectively. Also, it can be concluded that for a constant value of C_D (for example C_D = 7.801) the structure with FGX is under damped while about the other distribution

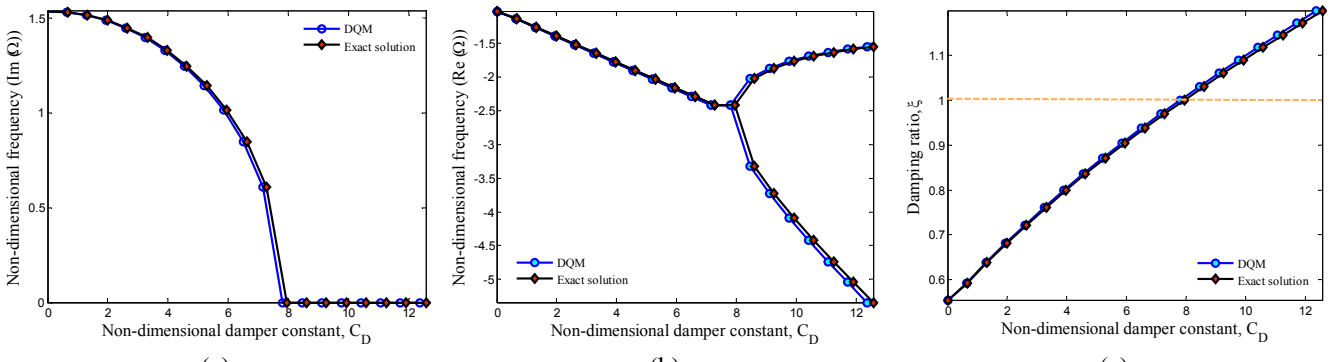

(a) (b) (c)

Fig. 2 Comparison of result obtained by DQM and exact solution (a) imaginary part of eigenfrequency; (b) real part of eigenfrequency; (c) damping ratio

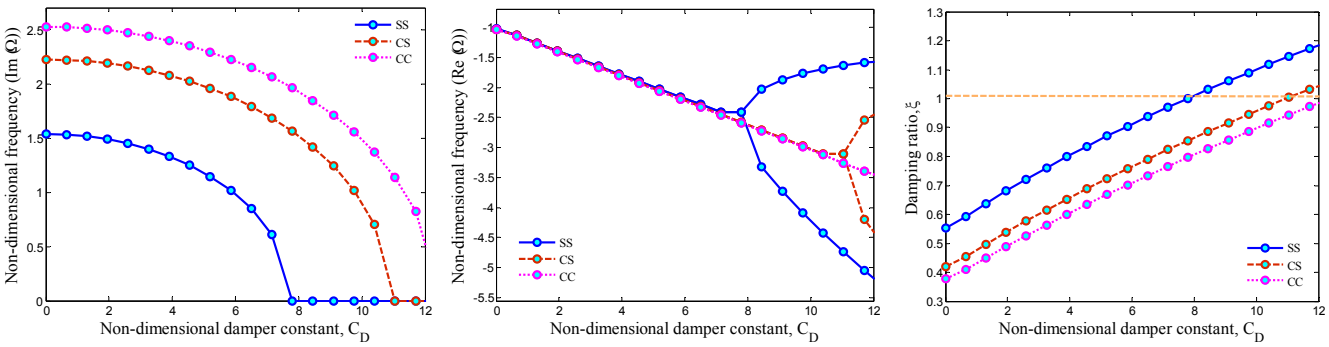

(a) (b) (c)

Fig. 3 Boundary condition effects on the (a) imaginary part of eigenfrequency; (b) real part of eigenfrequency; (c) damping ratio

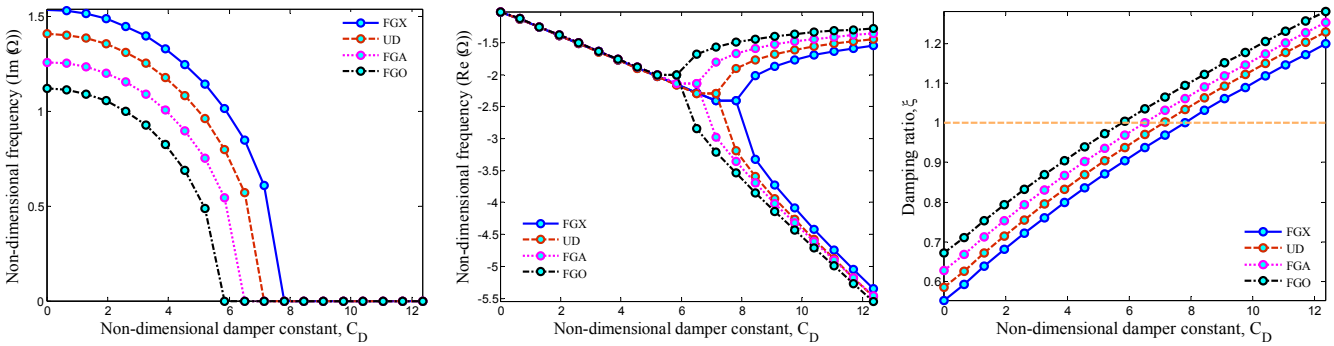

(a) (b) (c)

Fig. 4 Distribution type of CNTs effects on the (a) imaginary part of eigenfrequency; (b) real part of eigenfrequency; (c) damping ratio

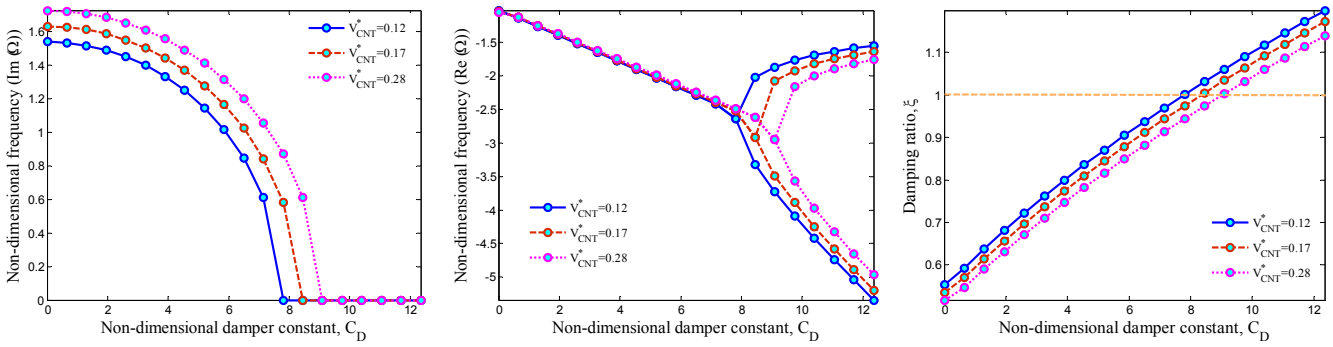

(a) (b) (c)

Fig. 5 Volume percent of CNTs effects on the (a) imaginary part of eigenfrequency; (b) real part of eigenfrequency; (c) damping ratio

types, the structure is critically damped or over-damped.

Variation of the imaginary and real parts of the eigen-frequency as well as damping ratio versus the volume percent of CNTs is illustrated in Fig. 5. As expected, with increasing the volume percent of CNTs, the stiffness of the structure increases and thus, the frequency grows up. As it can be seen, with increasing the volume percent of CNTs, the over-damped system transforms to the under-damped one and the critically damped situation occurs at higher values of damper constant.

Fig. 6 shows the effect of thickness to material length scale parameter ratio on the eigenfrequency of the system. It is obvious that with increasing the thickness to material length scale parameter ratio, the effect of size-scale becomes less significant and gets smaller. So, as this ratio increases, the stiffness of the structure decreases and as a result, system is critically damped and over damped for lower values of C_D.

The effect of magnetic field on the eigenfrequency and damping ratio of the system is probed in Fig. 7. From Fig. 7(a), it can be found that applying the magnetic field increases the imaginary part of the eigenfrequency because

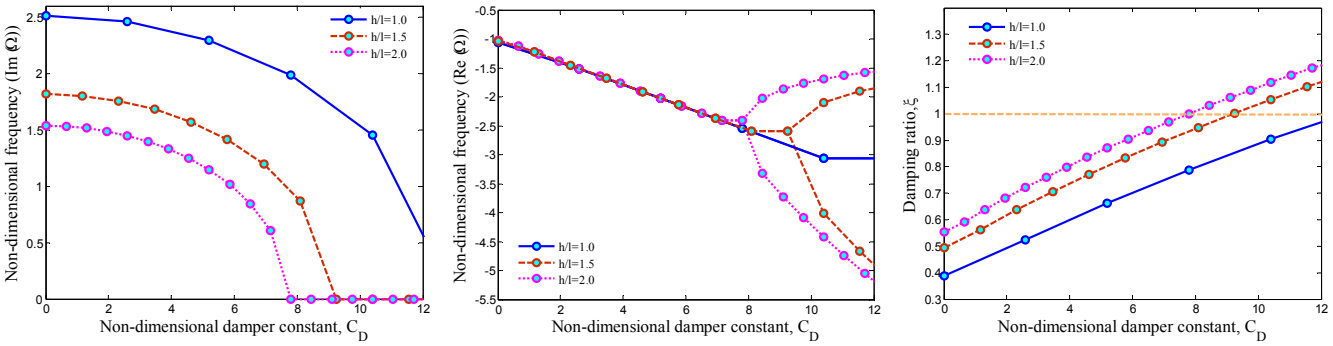

(a) (b) (c)

Fig. 6 Curved beam thickness to material length scale parameter ratio effects on the (a) imaginary part of eigenfrequency; (b) real part of eigenfrequency; (c) damping ratio

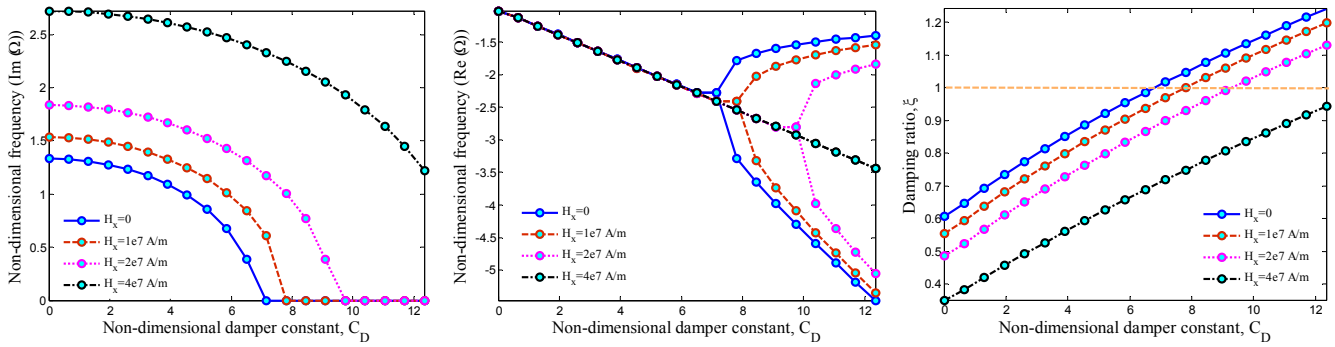

(a) (b) (c)

Fig. 7 Magnetic field effects on the (a) imaginary part of eigenfrequenc;. (b) real part of eigenfrequency; (c) damping ratio

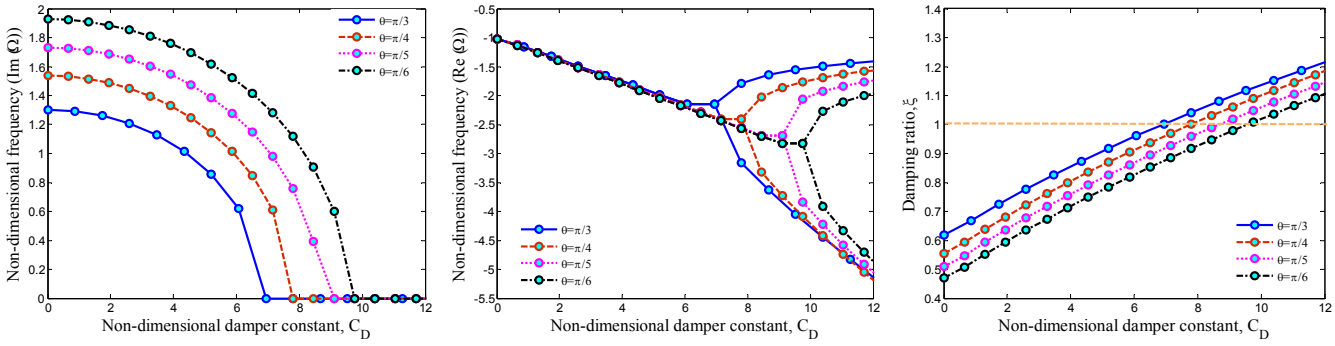

(a) (b) (c)

Fig. 8 Central angle of the curved microbeam effects on the (a) imaginary part of eigenfrequency; (b) real part of eigenfrequency; (c) damping ratio

the stiffness of the structure increases. In addition, it can be concluded from Fig. 7(b) that with increasing the magnetic field, the real part of the eigenfrequency curves intersect at the higher values of damper constant and thus the system will be in critically damped situation for higher values of damper constant. On the other hand, with applying the magnetic, the over-damped system transforms to the under-damped one as the damper constant increases (see Fig. 7(c)).

Variation of the eigenfrequency and damping ratio for different values of the central angle of the curved microbeam is plotted in Fig. 8. It can be seen that increasing the central angle decreases the frequency of the system. Also, with increasing the central angle of the curved microbeam, the critically damped situation occurs at lower values of damper constant. It means that with the decrement of the central angle, the system becomes more stable.

Fig. 9 shows the effect of temperature change on the imaginary and real parts of the eigenfrequency and damping ratio of the curved microbeam. As expected, increasing temperature decreases the frequency of the structure. The reason is that with increasing temperature, the mechanical,

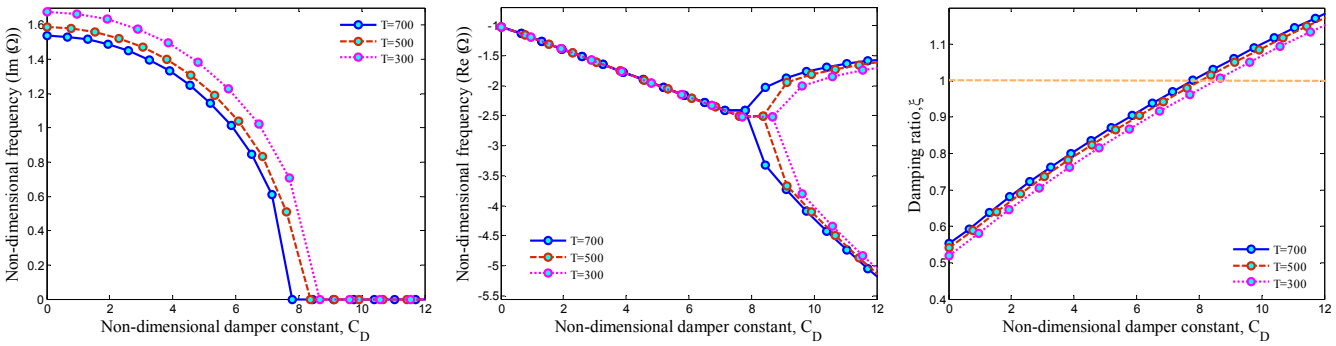

(a) (b) (c)

Fig. 9 Temperature change effects on the (a) imaginary part of eigenfrequency; (b) real part of eigenfrequency; (c) damping ratio

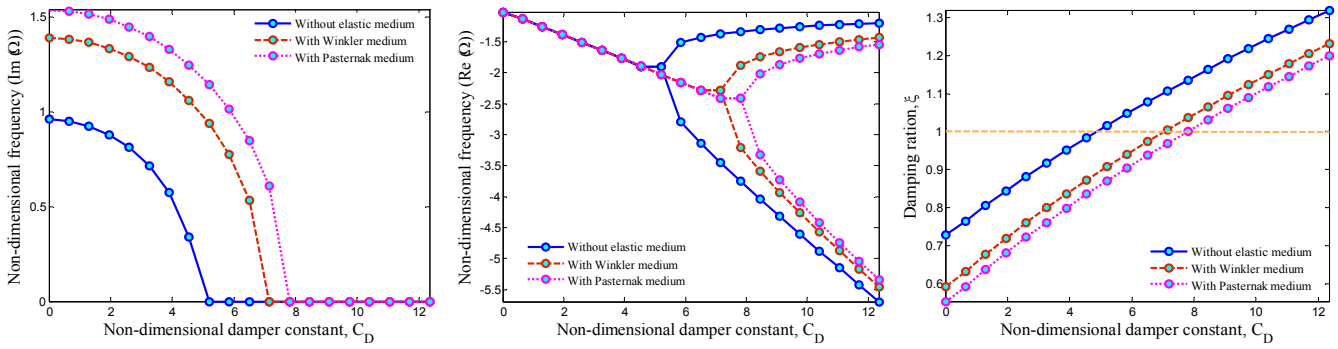

(a) (b) (c)

Fig. 10 Elastic medium type effects on the (a) imaginary part of eigenfrequency; (b) real part of eigenfrequency; (c) damping ratio

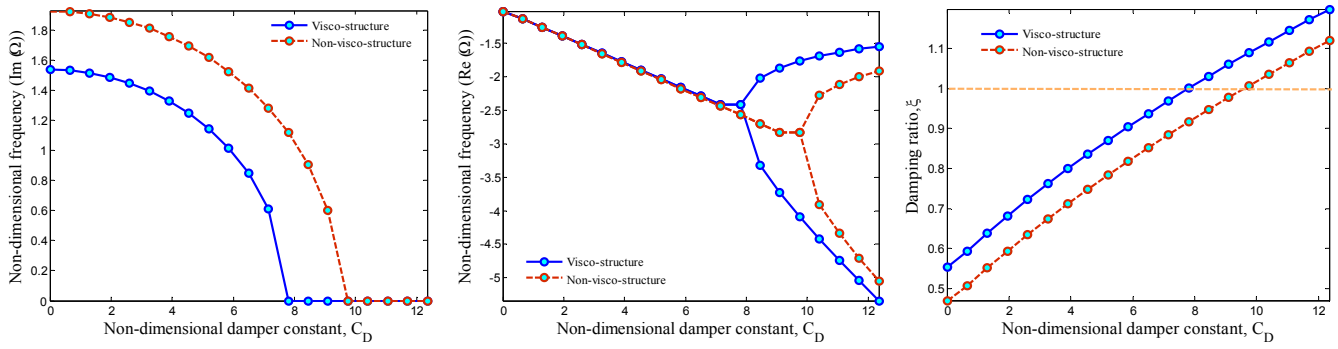

(a) (b) (c)

Fig. 11 Structural damping effects on the (a) imaginary part of eigenfrequency; (b) real part of eigenfrequency; (c) damping ratio

properties of the structure decreases and thus the stiffness of the system lessens. Furthermore, as temperature increases the critically damped situation happens at lower values of the damper constant.

The effect of the elastic medium is examined by plotting Fig. 10. As can be seen, considering the elastic medium leads to an increase in the stiffness of the structure and thus the frequency of the system increases. Moreover, the structure with the Pasternak medium has the highest stiffness with respect to Winkler medium. In addition, studying the real part of the eigenfrequency and damping ratio shows that with considering the elastic medium, the critically damped situation occurs at higher values of damper constant.

The variation of the eigenfrequency and damping ratio of the structure versus the structural damping for different values of damper constant is shown in Fig. 11. As can be seen, considering the structural damping leads to the increase of the frequency. Also, the non-visco-structure is critically damped at the higher values of the damper

constant with respect to the visco-structure.

6. Conclusions

In this paper, the vibration and damping behaviors of a FG-CNTs-reinforced composite curved microbeam were studied. The structure was considered to be subjected to a longitudinal magnetic field. Timoshenko beam theory was used to extend the mathematical model of the structure. In addition, the surrounding viscoelastic medium was simulated by normal springs, damper and shear elements. Applying strain gradient theory, the small scale effects were considered by three material length scale parameters. The extended rule of mixture was employed to obtain the effective material properties of the composite curved beam. The governing equations of the structure were derived based on Hamilton's principle and the imaginary and real parts of the eigenfrequency of the system were obtained using DQM. The effects of various parameter such as volume percent and distribution type of CNTs, temperature change, magnetic field, boundary conditions, material length scale parameter, central angle, viscoelastic medium and structural damping were examined. Numerical results show that the structure with SS or CS boundary condition was critically damped at the lower values of damper constant with respect to the structure with CC boundary condition. It was deduced that for a constant value of C_D the structure with FGX was under damped while about the other distribution types the structure was critically damped or over-damped. With increasing the volume percent of CNTs, the over-damped system transforms to the under-damped one and the critically damped situation occurs at higher values of damper constant. It was found that applying the magnetic field increases the imaginary part of the eigenfrequency because the stiffness of the structure increases. In addition, with increasing the central angle of the curved microbeam, the critically damped situation occurs at lower values of damper constant. Furthermore, considering the elastic medium leads to an increase in the stiffness of the structure and thus the frequency of the system increases. Moreover, the non-visco-structure was critically damped at the higher values of the damper constant with respect to the visco-structure.

References

Abdollahi, D., Ahdiaghdam, S., Ivaz, K. and Shabani, R. (2016), "A theoretical study for the vibration of a cantilever microbeam as a free boundary problem", *Appl. Math. Model.*, **40**(3), 1836-1846.

Ahouel, M., Houari, M.S.A., Adda Bedia, E.A. and Tounsi, A. (2016), "Size-dependent mechanical behavior of functionally graded trigonometric shear deformable nanobeams including neutral surface position concept", *Steel Compos. Struct., Int. J.*, **20**(5), 963-981.

Ansari, R., Gholami, R. and Sahmani, S. (2011), "Free vibration analysis of size-dependent functionally graded microbeams based on the strain gradient Timoshenko beam theory", *Compos. Struct.*, **94**(1), 221-228.

Chen, X. and Meguid, S.A. (2015), "On the parameters which govern the symmetric snap-through buckling behavior of an initially curved microbeam", *Int. J. Solids Struct.*, **66**, 77-87.

Dehrouyeh-Semnani, A.M., Dehrouyeh, M., Torabi-Kafshgari, M. and Nikkhah-Bahrami, M. (2015), "An investigation into size-dependent vibration damping characteristics of functionally graded viscoelastically damped sandwich microbeams", *Int. J. Eng. Sci.*, **96**, 68-85.

Ebrahimi, F. and Salari, E. (2015), "Thermal buckling and free vibration analysis of size dependent Timoshenko FG nanobeam in thermal environments", *Compos. Struct.*, **128**, 363-380.

Ghadiri, M. and Shafiei, N. (2016), "Vibration analysis of rotating functionally graded Timoshenko microbeam based on modified couple stress theory under different temperature distributions", *Acta Astronaut.*, **121**, 221-240.

Ghayesh, M.H., Farokhi, H. and Hussain, S.H. (2016), "Visco-elastically coupled size-dependent dynamics of microbeams", *Int. J. Eng. Sci.*, **109**, 243-255.

Ghayesh, M.H., Farokhi, H. and Gholipour, A. (2017), "Vibration analysis of geometrically imperfect three-layered shear-deformable microbeams", *Int. J. Mech. Sci.*, **122**, 370-383.

Ilkhani, M.R. and Hosseini-Hashemi, S.H. (2016), "Size dependent vibro-buckling of rotating beam based on modified couple stress theory", *Compos. Struct.*, **143**, 75-83.

Jia, X.L., Ke, L.L., Feng, C.B., Yang, J. and Kitipornchai, S. (2015), "Size effect on the free vibration of geometrically nonlinear functionally graded micro-beam under electrical actuation and temperature change", *Compos. Struct.*, **133**, 1137-1148.

Kolahch, R. and Moniribidgoli, A.M. (2016), "Size-dependent sinusoidal beam model for dynamic instability of single-walled carbon nanotubes", *Appl. Math. Mech. – Engl Ed.*, **372**, 265-274.

Kolahchi, R., Rabani Bidgoli, M., Beygipoor, Gh. and Fakhar, M.H. (2015), "A nonlocal nonlinear analysis for buckling in embedded FG-SWCNT-reinforced microplates subjected to magnetic field", *J. Mech. Sci. Tech.*, **29**, 3669-3677 .

Kolahchi, R., Hosseini, H. and Esmailpour, M. (2016a), "Differential cubature and quadrature-Bolotin methods for dynamic stability of embedded piezoelectric nanoplates based on visco-nonlocal-piezoelasticity theories", *Compos. Struct.*, **157**, 174-186.

Kolahchi, R., Safari, M. and Esmailpour, M. (2016b), "Dynamic stability analysis of temperature-dependent functionally graded CNT-reinforced visco-plates resting on orthotropic elastomeric medium", *Compos. Struct.*, **150**, 255-265.

Kolahchi, R., Zarei, M.Sh., Hajmohammad, M.H. and Naddaf Oskouei, A. (2017), "Visco-nonlocal-refined Zigzag theories for dynamic buckling of laminated nanoplates using differential cubature-Bolotin methods", *Thin-Wall Struct.*, **113**, 162-169.

Lam, D.C.C., Yang, F., Chong, A.C.M., Wang, J. and Tong, P. (2003), "Experiments and theory in strain gradient elasticity", *J. Mech. Phys. Solids*, **51**(8), 1477-1508.

Liu, Y.P. and Reddy, J.N. (2011), "A nonlocal curved beam model based on a modified couple stress theory", *Int. J. Struct. Stab. Dyn.*, **11**(3), 495-512.

Shafiei, N., Mousavi, A. and Ghadiri, M. (2016), "Vibration behavior of a rotating non-uniform FG microbeam based on the modified couple stress theory an GDQEM", *Compos. Struct.* **149**, 157-169.

Shen, H.Sh. and Zhang, Ch.L. (2011), "Nonlocal beam model for nonlinear analysis of carbon nanotubes on elastomeric substrates", *Comput. Mat. Sci.*, **50**(3), 1022-1029.

Şimşek, M. (2011), "Forced vibration of an embedded single-walled carbon nanotube traversed by a moving load using nonlocal Timoshenko beam theory", *Steel Compos. Struct., Int. J.*, **11**(1), 59-76.

Şimşek, M. (2014), "Large amplitude free vibration of nanobeams with various boundary conditions based on the nonlocal elasticity theory", *Compos. Part B: Eng.*, **56**, 621-628.

Şimşek, M. (2015), "Size dependent nonlinear free vibration of an axially functionally graded AFG microbeam using He's variational method", *Compos*. *Struct*., **131**, 207-214.

Tang, M., Ni, Q., Wnag, L., Luo, Y. and Wang, Y. (2014), "Size-dependent vibration analysis of a microbeam in flow based on modified couple stress theory", *Int*. *J*. *Eng*. *Sci*., **85**, 20-30.

Togun, N. and Bağdatli, S.M. (2016), "Size dependent nonlinear vibration of the tensioned nanobeam based on the modified couple stress theory", *Compos*. *Part B*: *Eng*., **97**, 255-262.

Wang, L., Xu, Y.Y. and Ni, Q. (2013), "Size-dependent vibration analysis of three-dimensional cylindrical microbeams based on modified couple stress theory: A unified trestment", *Int*. *J*. *Eng*. *Sci*., **68**, 1-10.

Wang, L., Liu, W.B. and Dai, H.L. (2015), "Dynamics and instability of current-carrying microbeams in a longitudinal magnetic field", *Physica E*, **66**, 87-92.

Yang, W.D., Fang, C.Q. and Wang, X. (2017), "Nonlinear dynamic characteristics of FGCNTs reinforced microbeam with piezoelectric layer based on unifying stress-strain gradient", *Compos*. *Part B*: *Eng*., **111**, 372-386.

Zamanian, M. and Karimiyan, A. (2015), "Analysis of the mechanical behavior of a doubled microbeam configuration under electrostatic actuation", *Int*. *J*. *Mech*. *Sci*., **93**, 82-92.

Zenkour, A.M. and Abouelregal, A.E. (2016), "Thermoelastic interaction in functionally graded nanobeams subjected to time-dependent heat flux", *Steel Compos*. *Struct*., *Int*. *J*., **18**(4), 909-924.

Zhang, L.W., Lei, Z.X. and Liew, K.M. (2015), "Free vibration analysis of functionally graded carbon nanotube-reinforced composite triangular plates using the FSDT and element-free IMLS-Ritz method", *Compos*. *Struct*., **120**, 189-199.

CC